Regina Eckhard, BSc

Ultra-high performance concrete dies for deep drawing of high-strength steels

Master's Thesis

To achieve the university degree of

Diplom-Ingenieurin/Master of Science

Master's degree program: Production Science and Management

submitted to

Graz University of Technology

Supervised by

Univ.-Prof. Dipl.-Ing. Dr.techn. Christof Sommitsch

Dipl.-Ing. Vladimir Bošković

Performed in

Institute of Materials Science, Joining and Forming

Research Group Tools & Forming

Graz, September 2017

Affidavit

I declare that I have authored this thesis independently, that I have not used other than the declared sources/resources, and that I have explicitly indicated all material which has been quoted either literally or by content from the sources used. The text document uploaded to TUGRAZonline is identical to the present master‘s thesis dissertation.

…… ……

Date Signature

Eidesstattliche Erklärung

Ich erkläre an Eides statt, dass ich die vorliegende Arbeit selbstständig verfasst, andere als die angegebenen Quellen/Hilfsmittel nicht benutz, und die den benutzten Quellen wörtlich und inhaltlich entnommenen Stellen als solche kenntlich gemacht habe. Das TUGRAZonline hochgeladene Textdokument ist mit der vorliegenden Diplomarbeit identisch.

…… ……

Datum Unterschrift

Acknowledgement

First of all I would like to thank all my colleagues from the Research Group Tools & Forming of the Institute of Material Science, Joining and Forming at the Graz University of Technology, who supported me with their knowledge during the entire time of my master thesis. Further I would like to thank Univ.-Prof. Dipl.-Ing. Dr.techn. Christof Sommitsch for the supervision and the assessment of the thesis. Special thanks to Dipl.-Ing. Vladimir Bošković and DDDipl.-Ing. Dr. mont. Josef Domitner, who advised and supported me with their technical knowledge. I like to thank the whole workshop team, who was irreplaceable during the production of the mold and especially Mr. Nino Müllner for his additional support during the tests.

Furthermore, I would like to thank Priv.-Doz. Dipl-Ing. Dr.techn. Bernhard Freytag and Mr. Hannes Koitz from the Laboratory for Structural Engineering and Dipl-Ing. Dr.techn. Joachim Juhart from the Institute of Technology and Testing of Construction Materials for their support and knowledge. Without their support this thesis would not have been possible.

I like to thank the MAGNA Cosma Engineering Europe GmbH, specially DI Christian Juricek and DI, IWE Mustafa Kicin, who made the project possible and for their support.

Last but not least I would like to thank my family, who supported me my whole life and always believed in me, even if I did not. In particular I would like to thank my parents, who not only supported me in my decisions but also gave me strength to accomplish my goals.

Abstract

Most of the investigations in the sheet metal forming area are focusing on using even harder and/or lighter sheet metal. Only a few researchers address their studies to the needed tool material for the forming process.

In this thesis, ultra-high-performance concrete (UHPC) is under investigation as a possible alternative for tool steel. In comparison to normal strength concrete, this UHPC has a much higher strength thus making it possible to construct much more delicate structures. Given the fact, there is only low shrinkage of the concrete volume which stops after a heat treatment of approximately 48 hours, UHPC shows the necessary shape stability to ensure a stable forming process.

The objective of this thesis is to find out if wear resistance is sufficient to use the concrete in prototyping. Therefore, a punch of a deep drawing tool, with a cup geometry, was produced using UHPC and tested for wear with adequate number of strokes.

Kurzfassung

Die meisten Untersuchungen im Bereich Blechumformung beziehen sich auf die Verwendung von noch härteren und/oder leichteren Blechen. Nur wenige befassen sich mit dem für das Werkzeug benötigten Material für den Umformprozess.

In dieser Arbeit wird ultra-hochfester Beton (UHPC) als Alternative zu Werkzeugstahl untersucht. UHPC kann im Vergleich zu normalem Beton viel höhere Kräfte ertragen und lässt sich in feineren Strukturen darstellen. Auf Grund der Tatsache, dass die Schrumpfung des Betonvolumens nur gering und nach einer Wärmebehandlung von ca. 48 Stunden beendet ist, kann die benötigte Formerhaltung für einen stabilen Umformungsprozess gewährleistet werden.

Ziel der Arbeit ist es, herauszufinden ob die Verschleißfestigkeit des Betons ausreichend ist, um ihn im Prototypenbau anwenden zu können. Hierfür wurde der Stempel eines Tiefziehwerkzeuges mit einer Napf Geometrie aus UHPC hergestellt und auf Verschleiß mittels einer entsprechenden Anzahl von Hüben getestet.

Table of Contents

1 Introduction

The civil and the mechanical engineering department at the Graz University of Technology were both created within 60 years after the founding of the University in 1811[1]. Hence, it was only a matter of time until these two fields recognized the potential and started combining their knowledge. The first industries which come to mind when thinking about these two fields of study are the automotive and the construction industry, where concrete and steel are the most used materials.

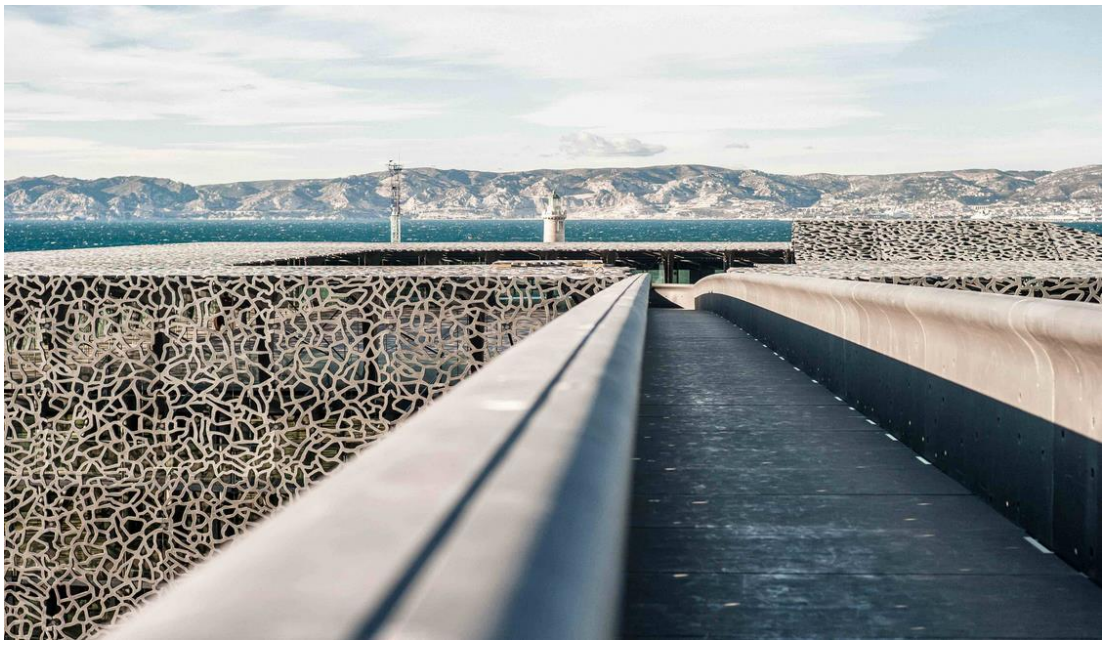

Figure 1.1: MuCEM, Ductal® Lattice & Structural Element Solutions, Marseilles France[2]

The concrete industry has made remarkable progress over the last decades. The concrete which non-civil engineers mostly know is far away from the highly advanced materials the institutes at universities are researching. The research progresses can be seen in countless and impressive constructions of buildings, bridges and monuments, such as the construction shown in Figure 1.1. In 1988 the highest

[1] cf. history.tugraz.at

[2] ductal.com

compression strength class described in DIN 1045 was only B55 (which is a compression strength of approximately 45 N/mm^2), whereas compressive strengths of up to 200 N/mm^2 and bending tensile strengths of 50 N/mm^2 are now possible. Therefore, this concrete can absorb intended tensile strengths for the first time.[3] With these remarkable changes in the quality of this brittle material, applications in the mechanical engineering area are now possible.

On the other side of this cooperation is the fast moving automotive industry. In 1974 the legendary VW Golf I was introduced, replacing the VW Bug, which was built based on a concept from the 1930s.[4] In the past 30 years "time to market" of a new automobile shrunk rapidly. In the 1980s a car manufacturer had 6 years on average until the ramp up of production should be finished, nowadays this time frame lies between 4 and 2.5 years for the module set up.[5] Therefore prototype production needs to be as efficient and adaptable as possible.

This need for a fast and cost efficient prototyping is the reason to consider other materials than steel for sheet metal forming tools. Because of breakthroughs in concrete development in the past decades and the resulting advantages of this material, it has become a considerable alternative to the commonly used steel.

1.1 Objectives of this thesis

This thesis focuses on verifying the usability of an ultra-high-performance concrete in the deep drawing process for the prototype construction in the automotive industry. It was agreed upon with the project partner, MAGNA Cosma Engineering Europe GmbH to set the specifications of the work after a literature research and meetings with the Laboratory for Structural Engineering (LKI) of the Graz University of Technology.

The subjects to be investigated were, whether to perform cold, warm or hot forming tests and what blank material to use. Therefore, existing applications of concrete in

[3] cf. Fehling, E., et. al. (2013), p. 121

[4] cf. bundestag.de

[5] cf. Bischoff, R. (2007), p. 2

the forming technology and a thorough research on the mechanical properties of the ultra-high-performance concrete was conducted.

After the research and design of the experiment were completed, the practical investigation of the concrete part was performed on the hydraulic press at the research group Tools and Forming of the Institute of Material Science, Joining and Forming of the Graz University of Technology. To be able to make a valid statement about the abilities of the concrete punch at least 250 strokes with resulting parts of adequate quality needed to be endured by the punch without much wear.

The unknown variables in finding the right parameters of the deep drawing process were not only the behavior of the blank material, but also the material of the punch, the concrete. Therefore, it was decided on a known deep drawing material for the blanks, DC04, where only small adaptations of the parameters needed to be done.

A non-destructive investigation of the concrete punch needed to be done before and after the deep drawing tests, to be able to outline the wear behavior of the material.

The results of both paper study and practical investigation are discussed in the following thesis.

2 Theoretical background

This study focuses on the deep drawing process, especially tool fabrication and ultra-high-performance concrete as a possible steel substitute. This chapter gives all the necessary information for the understanding of the project.

2.1 Deep drawing

Deep drawing is a forming process described in DIN 8584: Deep drawing is a compression and tension forming process of a cut (metal) sheet into a hollow body where one side is open, without willingly changing the sheet thickness.[6] Figure 2.1 depicts all the forming processes described in the different DIN norms.

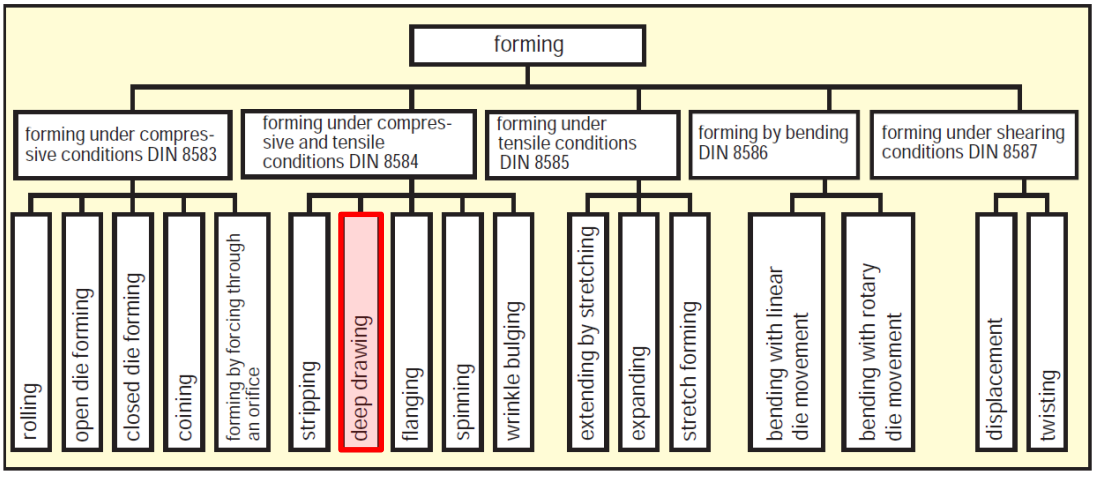

Figure 2.1: Classification of production processes used in forming[7]

The deep drawing process can be performed with a rigid tool (consisting of a die and a punch), a flexible tool (consisting of a punch and a rubber pad), an action medium (liquids, gasses) or an active energy (magnetic field).[8]

[6] cf. Fritz, A.H. (2015), p.473

[7] Schuler (1998), p. 7

[8] cf. Westkämper, E. and Warnecke, H.-J. (2010), p. 110

The principle of the deep drawing process, used in this thesis, is shown in Figure 2.2. The tool consists of a punch, a draw ring and a blank holder. The blank gets fixed with the blank holder force F_N between the draw ring, allowing the blank holder and the punch to form the sheet into the wanted shape.

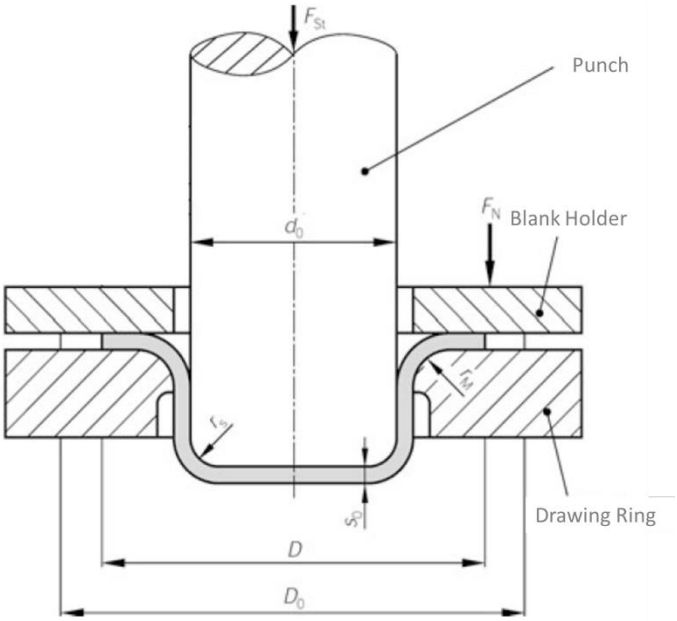

F_{St} punch force

F_N blank holder force

d_0 diameter of the punch

D_0 blank diameter

D current blank diameter

r_s punch radius($\approx 0.15 * d_0$)

s_0 blank thickness

r_M drawing ring radius ($\approx 8 * s_0$)

Figure 2.2: Scheme of the deep drawing process[9]

Deep drawing is a process of indirect force transmission. The necessary drawing force F_{St} is transmitted from the punch to the bottom of the deep drawing part and forwarded by the cup wall to the flange.[9]

The resulting stresses and strains in different parts of the formed blank are shown in Figure 2.3.

[9] cf. Fritz, A. H. (2015), p. 474

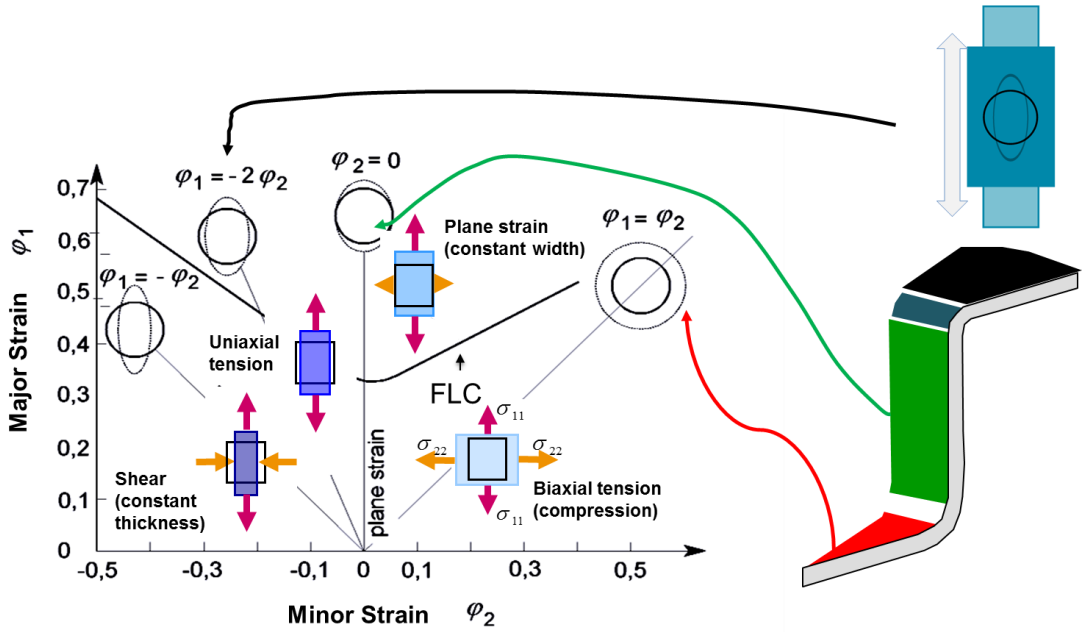

Figure 2.3: Deformation during the deep drawing process[10]

Geometry of the blank[11]

In case of deep drawing of rotationally symmetric metal forming parts, the surface of the formed part is as big as the initial blank. Therefore, the blank diameter D_0 is depending on the punch diameter d_0, and the maximal deep drawing depth at full pullthrough h_{max}.

$$D_0 = \sqrt{4 * d_0 * h_{max} + d_0^2}$$

Equation 2.1: Blank diameter for a rotationally symmetric part

Deep drawing tool

The design of the deep drawing tool depends on the special features of the geometry and the material of the deep drawn part and the forming process itself, if it is cold,

[10] cf. Doege, E. and Behrens, B.-A. (2010), p. 311

[11] cf. Siegert, K. (2015), p.104

warm or hot forming.[12] The following specifications of the deep drawing tool refer to a cold forming process with a simple cup geometry, as used in the experiment.

A widely-used material in building forming tools is steel. Especially for deep drawing tools the cold work steel called 90MnCrV8 (1.2842) is commonly used.[13] The chemical composition of this steel is listed in Table 2.1.

Table 2.1: Chemical composition of the tool steel[14]

C	Si	Mn	Cr	V
0.90	0.20	2.0	0.4	0.1

This tool material has a strength of 760 N/mm^2 and a thermal conductivity of 33 W/m*K.[14]

Fabrication of the tool

The fabrication of the tool starts with milling the wanted geometry out of a steel block of the chosen material. Afterwards a thorough surface treatment of those surfaces subjected to friction is very important. These surfaces have to be grinded, lapped and polished after hardening and tempering of the tool.[15]

2.2 Ultra-high-performance concrete (UHPC)

Ultra-high-performance concrete, or in further reference known as UHPC, is characterized with a very dense structure and a compressive strength of approximately 200 N/mm^2, which is higher than the highest compressive strength

[12] cf. Klocke, F. and König, W. (2006), p.346

[13] cf. Klocke, F. and König, W. (2006), p.107

[14] meusburger.com

[15] cf. Klocke, F. and König, W. (2006), p.348

class of DIN EN 206-1 for high performance (normal) concrete.[16] When reinforced with high strength steel fibers, the concrete reaches tensile strengths of more than 15 N/mm^2,[17]whereas unreinforced concrete can only reach between 7 and 11 N/mm^2 [18]. It can be produced as a fine concrete with a maximal grain size of 0.5 mm or even with a grain size up to 16 mm.[19] These special properties of UHPC result in the combination of tightly packed ultrafine particles and an extremely low water/binder ratio of about 0.2.[17]

2.2.1 Components

Commonly used concrete is usually a mixture of cement, water, sand and other additives such as fly ash[20] ultra-high-performance concrete on the other hand has a more complicated composition as shown in Figure 2.4.

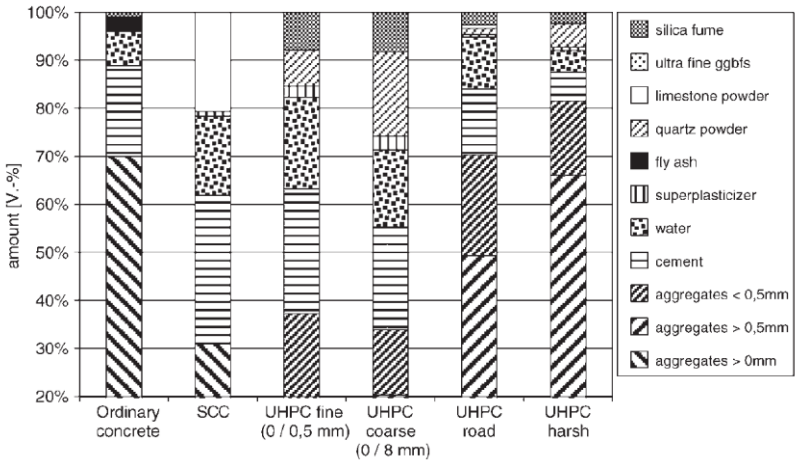

Figure 2.4: Comparison of the mixtures of various types of concretes[21]

[16] cf. Schmidt, M., et al. (2007), p.1

[17] cf. Fehling, E., et al. (2014), p.5

[18] cf. Fehling, E., et al. (2013), p.136

[19] cf. Schmidt, M. (2003), p. 5

[20] cf. Moro, J. L., et al. (2009), p.154

[21] Fehling, E., et al. (2014), p.7

To give a more detailed idea of the complicated composition of the UHPC the basic recipe for a UHPC according to SPP 1182 is listed in Table 2.2.

Table 2.2: Basic recipe for the UHPC according to the SPP 1182[22]

Material	Unit	M2Q-fine grain	B4Q-coarse grain
Water	[kg/m³]	166	158
Cement	[kg/m³]	832	650
Silica Fume	[kg/m³]	135	177
Flow Agent PCE	[kg/m³]	29.4	30.4
Quartz Flour I	[kg/m³]	207	325
Quartz Flour II	[kg/m³]	0	131
Quartz Sand 0.125/0.5 mm	[kg/m³]	975	354
Basalt 2/8	[kg/m³]	0	597
Steel Fibers	[kg/m³]	195	195

In order to optimize the mixture of the concrete the water/ultrafine particle ratio (w/F_v) was introduced.

$$\frac{w}{F_v} = \frac{w}{\sum(c + ultrafine\ particles)_{vol}}$$

Equation 2.2: w/F_v ratio[17]

[22] cf. Sagmeister, B (2017), p. 32

With the w/F_v value the grading quality of the ultrafine particles and the characters of the pores, which have to be filled with water, can be measured. For instance, it is possible to increase the compressive strength of the UHPC by 30% by increasing the w/F_v value by only 3% while keeping the same w/c ratio. Furthermore, the required amounts of water and superplasticizer are dependent on the packing density of the dry components, which is reduced with rising density.[23]

Cement

Cement is one of the most important components of concrete, as the water/cement-ratio (w/c-ratio) is essential for the mechanical properties of the concrete. It is building the matrix in which the aggregates are embedded.

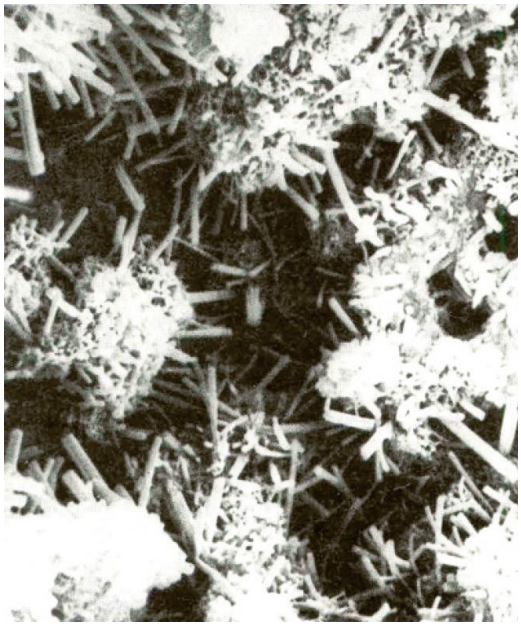

Figure 2.5: Material structure of concrete[24]

[23] cf. Fehling, E., et al. (2014), p.8-10

[24] Moro, J. L., et al. (2009), p.155

Over the years, the low-alkali Portland cement CEM I, with a high sulfate resistance and a low hydration heat, has become the most used cement for UHPC. Its advantages are limited water usage and chemical shrinkage and furthermore the possibility of excluding an alkali-silica-reaction.[25]

The main materials needed for the production of Portland cement are chalk or limestone and clay, which consist mostly of lime, silica, alumina and iron oxide.[26] The major constituents are shown in Figure 2.6.

Bezeichnung des reinen Minerals	Formel	Abkürzung	Bezeichnung des im Klinker vorliegenden Minerals
Tricalciumsilicat	$3\ CaO \cdot SiO_2$	C_3S	Alit
Dicalciumsilicat	$2\ CaO \cdot SiO_2$	C_2S	Belit
Tricalciumaluminat	$3\ CaO \cdot Al_2O_3$	C_3A	Aluminat
Calciumaluminatferrit	$4\ CaO \cdot Al_2O_3 \cdot Fe_2O_3$	$C_2(A,F)$	Aluminatferrit

Figure 2.6: Main phases of Portland cement clinker[27]

Water

The next important component is the second part of the w/c-ratio, the water. Water is the chemical reaction partner of the binder, which is cement[28]. The amount of water used in the concrete mix is essential for the strength and the flowability of the concrete, which will be discussed in the following paragraphs.

[25] cf. Fehling, E., et al. (2013), p.125-126

[26] cf. Lyons, A. (2006), p.52

[27] Stark, J., Wicht, B. (2013), p.29

[28] cf. Sagmeister, B. (2017), p.2

Reactive additives

Silica fume

Silica fume is worldwide available by different sources, because it is a by-product of the steel manufacturing process and therefore it fluctuates in quality.[29] Silica fume is physically used as a micro filler in the concrete. During the heat treatment of the concrete it is part of the creation of additional firmness-forming hydrate phases. The added silica fume should at least consist of 96 M.-% of amorphous SiO2 and only a little amount of carbon, because carbon increases the usage of water and flow agents.[30] The amount of silica fume must be at least as much as needed to fill the pores, because otherwise the viscosity of the concrete can become too high. Consequently, if the minimal quantity of silica fume is not used, the optimization of the package density will become redundant.[31]

Granulated slag

It is possible to further reduce the needed water and flow agent of the UHPC by replacing some of the CEM I with ground granulated slag, without losing any advantages.[30]

Inert additives

Usually fine quartz flours are used as an additive to get an optimal packing of the grain composition. Whereas, lime stone is not a good additive, because it is less hard and causes the concrete to be stickier and more tough.[32]

[29] cf. Sagmeister, B. (2017), p.31

[30] cf. Fehling, E., et al. (2013), p.126-127

[31] cf. Fehling, E., et al. (2014), p.13

[32] cf. Fehling, E., et al. (2013), p.127

Flow agents

The flow agents for UHPC are based on polycarboxylat-ethers (PCE), especially for UHPCs with a high portion of silica fume. They are able to disagglomerate the cement and the other solid materials sufficiently.[32]

Steel fibers

Steel fibers are used to make the very rigid UHPC more durable for tensile forces. From experience we know they should have a maximum diameter of 0.2 mm, a length between 9 and 17 mm and a tensile strength of at least 2000 N/mm^2.[33]

The mechanical strength of fiber reinforced UHPC is dependent on the distribution of the steel fibers the better their distribution the better the properties of the UHPC. The allocation of added steel fibers is influencing the homogeneity of the UHPC. If yield stress and plastic viscosity of the concrete are not balanced, the fibers are not distributing uniformly and create clusters of fibers in the concrete matrix. This uneven placing of fibers can happen either during the mixing of the concrete or as a result from the stability of the UHPC mixture during the casting and the rheological performance of the fresh mortar matrix. [34]

2.2.2 Composition and mixing of the UHPC

The first step in designing a UHPC mix is to select and define the ultrafine materials for achieving an optimum packing density. After numerically optimizing the packing density, it needs to be experimentally validated. The goal is to reach the maximum w/F_v value while using the least amount of water and flow agent. Contrary to normal strength concrete the w/c value should not be varied overmuch during the mix design, because even small alterations above the maximum value of approximately 0.24 can cause the formation of capillary pores. These pores reduce the characteristic imperviousness of the microstructure, which results in the occurrence of drying

[33] cf. Fehling, E., et al. (2013), p.127-128

[34] cf. Wang, R., et al. (2017)

shrinkage and autogenous shrinkage. However, a small addition of water may enhance the effect of the flow agent.[35]

After selecting type and quantity of the components, the correct mixing process needs to be determined. The requisite to achieve the desired outcome is a mixing energy high enough to solubilize the ultrafine particles and to moisten the particles sufficiently with water and flow agent. Mixers with adjustable turning speed are of advantage, because different stages of the mixing process need different rotational speeds.[35]

At first, the dry components are put into the mixer and blended for 30 to 120 seconds. Afterwards the water is added and mixed into the dry materials. The next ingredient to be mixed in is the flow agent and lastly the steel fibers. The mixing time is dependent on the type of mixer, the size of the batch, the degree of filling the mixer, the temperature and most importantly the reaction time of the flow agent. Therefore, the timeframe of the blending lies between three and 15 minutes. At the end of the mixing process it has to be ensured that the desired texture has been reached.[36]

2.2.3 Heat curing

The low water content of UHPC causes the concrete to start curing during casting. As a result, a tough “elephant skin”, only a few tenths of a millimeter thick, starts to grow on uncovered surfaces and the concrete’s deaeration as well as its further leveling potential become limited. This effect can be avoided, by spraying curing agent or water on the affected surface immediately after casting and covering it with plastic sheeting. [37]

To ensure the high strength of the UHPC a heat treatment is applied. The cast parts are demolded after 24 hours to be heat treated at around 90°C for 48 hours. Because

[35] cf. Fehling, E., et al. (2014), p.15

[36] cf. Fehling, E., et al. (2014), p.15-17

[37] cf. Fehling, E., et al. (2014), p.17

of the low water content in the mixture, the concrete part needs to be protected from desiccation. Therefore, it is necessary to apply an airtight cover.[38]

The chemical hydration can be accelerated by heat curing, which results in a denser microstructure as more hydrated parts are formed to fill the pores and voids. This can be verified with the founding of Li et al. According to them, the most probable pore diameter measured in their experiment before heat curing was 31.90 nm and after curing of 10 and 48 hours approximately 10 nm. An additional founding was that the hydration of the UHPC finished after 10 hours of curing. [39]

2.2.4 Mechanical properties

One of the most common properties of concrete is its huge difference in pressure and tensile endurance, as shown in Figure 2.7. The stress-strain-curve of normal strength concrete shows the typical mineral curve shape which becomes curvier with a lower incline with increasing stress. The peak of the curve occurs at the breaking stress ($\sigma_B \approx 25$ N/mm^2).[40]

[38] cf. Fehling, E., et al. (2014), p.17-18

[39] cf. Li, W., et al. (2016)

[40] cf. Moro, J. L., et al. (2009), p.157-160

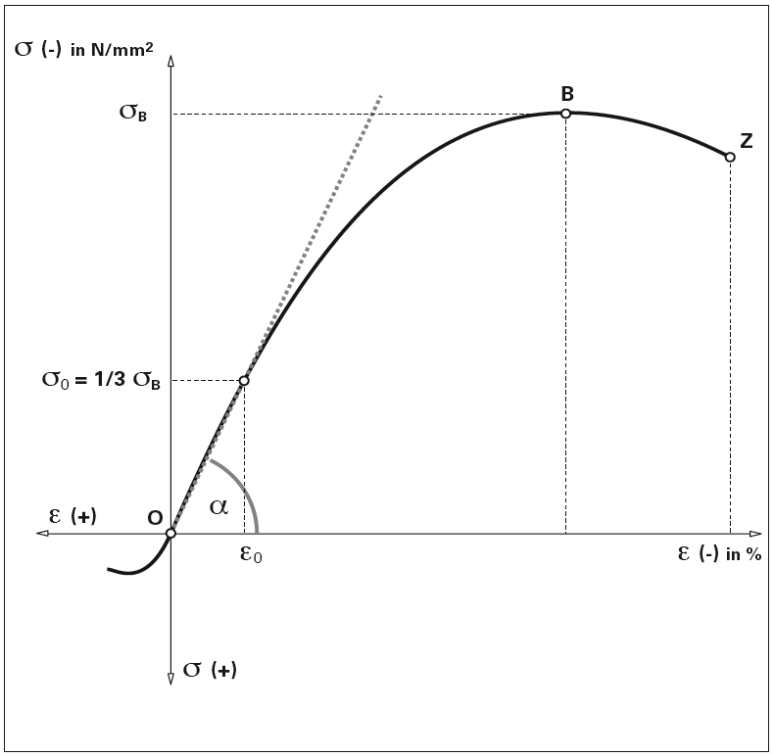

Figure 2.7: Stress-strain-diagram of normal-strength concrete[41]

UHPC, on the other hand, has a different breaking behavior than normal strength concrete, shown in Figure 2.8. The dense microstructure of UHPC has given the material high strength and greater stiffness, at cost of making the concrete more brittle.[42]

Pressure behavior

The stress strain curve of unreinforced UHPC, Figure 2.8, is more linear than that of normal strength concrete, Figure 2.7. This linear behavior changes shortly before reaching its maximum compressive strength, showing microcracks ant the start of failure. The failure of unreinforced UHPC is very sudden, it might even be described as explosive. [42]

[41] Moro, J. L., et al. (2009), p.157

[42] cf. Fehling, E., et al. (2014), p. 23

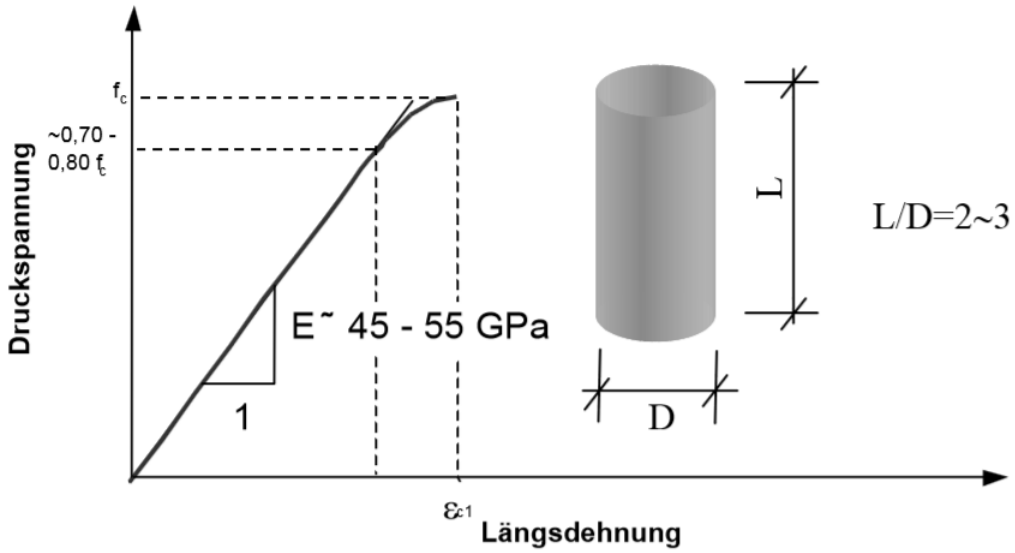

Figure 2.8: Compressive behavior of UHPC without fibers[43]

The addition of high strength steel is used to improve the post-peak structural behavior of the UHPC, shown in Figure 2.9. Reinforcement with fibers has an effect only on the descending portion of the curve not the ascending until an addition of more than 2.5 vol.% of fibers. Further, the value of improvement is immensely influenced by the following characteristics of the fibers:

- fiber content
- fiber geometry
- fiber orientation in the casted part
- conjunction of the fiber and the concrete matrix
- stiffness of the fibers

Therefore, the descending part of the stress strain curve is nearly impossible to predict, necessitating laboratory studies. This dependence on the amount of fibers and their characteristics, is shown in Figure 2.9.[44]

[43] Smidt, M., et al. (2007), p. 54

[44] cf. Fehling, E., et al. (2014), p. 23-26

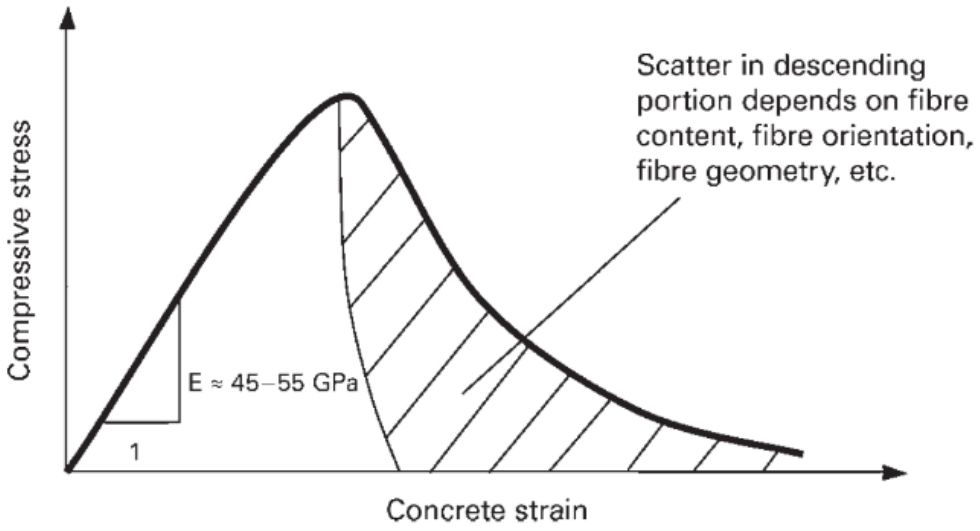

Figure 2.9: Compressive Behavior of UHPC with fibers[45]

Tensile behavior

The tensile strength of UHPC does not differ much from that of normal strength concrete, the typical value is between 7 and 11 N/mm^2. Without steel fibers, the tensile behavior can be influenced by adding silica fume to the UHPC matrix. The cracks of the UHPC are running through the grains of the aggregates and the edges of the cracks are very smooth. Therefore, it can be concluded that the interlocking effects of normal strength concrete are not present in the matrix of the UHPC.[46]

By reinforcing the matrix with high strength steel fibers, a different positive effect can be triggered. The rise of tensile strength endurance. The high strength steel fibers bridge over the cracks in the matrix and transfer some of the tensile stresses in favorable conditions. In Figure 2.10 the dependence of the post cracking behavior on the steel fibers is illustrated. [47]

[45] Fehling, E., et al. (2014), p. 26

[46] cf. Fehling, E., et al. (2014), p. 27-28

[47] cf. Fehling, E., et al. (2014), p. 28

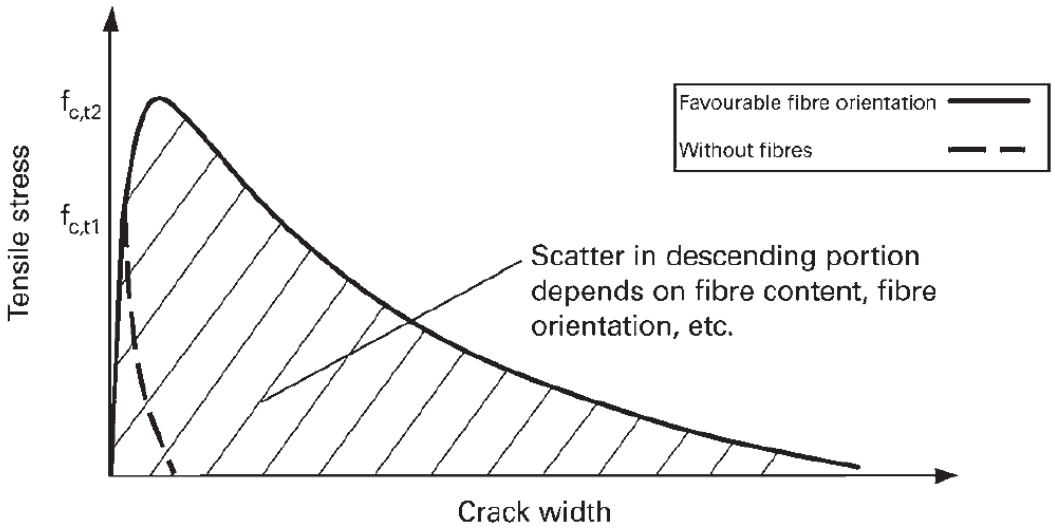

Figure 2.10: The stress-crack width behavior of UHPC, reinforced and not, in a tensile test[48]

Shrinkage

Concrete shrinks because of the chemical binding of water in cement stone. The constant need for moisture in concrete results in a volumetric shrinkage of the material. In case of a normal strength concrete, the decrease of volume happens slowly and is finished only years after casting the structural element.[49]

The shrinkage of UHPC proceeds much faster than that of normal strength concrete, as it stabilizes after 10 hours of heat curing at 90°C. [50] The process is finished after the usual 48 hours of the curing process.[51] Hence, the hydration of the concrete has also ended after the heat treatment. For an ultra-high-performance concrete the total shrinkage strain lies between 0.6 and 0.9 mm/m, depending on the mix composition.[52]

[48] Fehling, E., et al. (2014), p. 29

[49] cf. Moro, J. L., et al. (2009), p.156-157

[50] cf. Li, W., et al. (2016)

[51] cf. Fehling, E., et al. (2013), p. 130

[52] cf. Fehling, E., et al. (2014), p. 43

The stopping of shrinkage after heat curing at 90°C for 48 hours is illustrated in Figure 2.11, with a comparison to normal air-dried concrete at 20°C and 65% humidity.

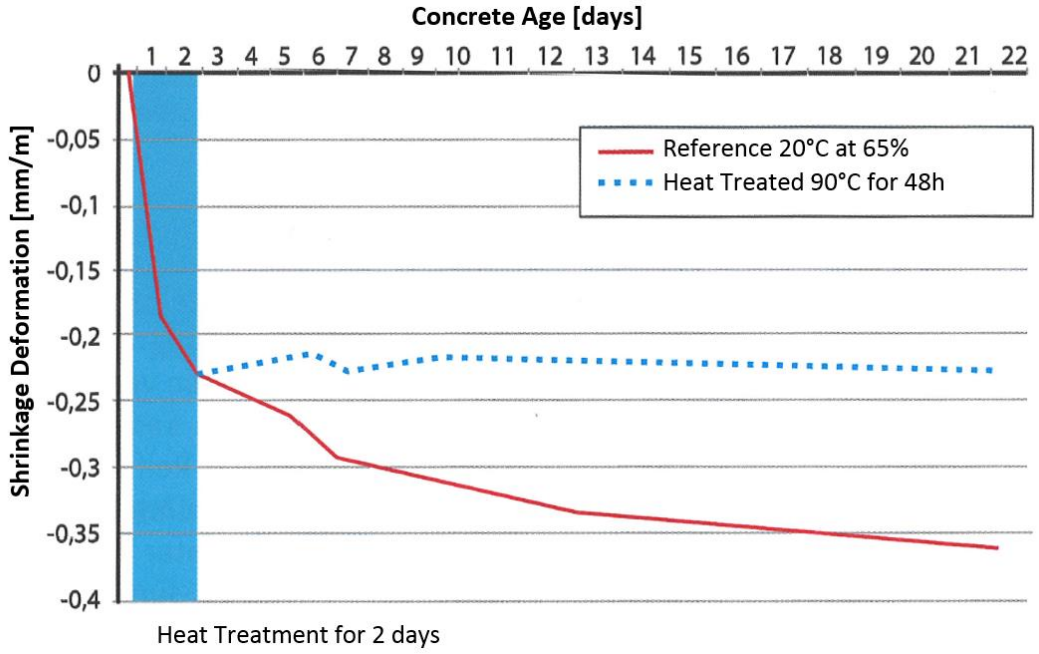

Figure 2.11: Shrinkage of air dried and heat cured concrete[53]

Creep

Creep of a material means that if a part is subjected to a compression force the part immediately deforms elastically. If the pressure is not released an additional plastic deformation happens. In other words, the material tries to escape from the load with creeping. The creep of concrete is dependent on the concrete age, the amount and duration of the load as well as the climatic conditions.[54]

Similar to the shrinkage of concrete, creep can also be extremely reduced with a heat treatment ($\varphi_{\text{without heat treatment}}$=0.6-1.4 and $\varphi_{\text{with heat treatment}}$=0.2-0.4). Due to the very compact microstructure capillary water gets hindered in its movement and therefore

[53] cf. Sagmeister, B. (2017), p.87

[54] cf. Sagmeister, B. (2017), p.91

the amount of creep resulting from drying is low compared to normal strength concrete.[55]

Abrasion behavior

The abrasion resistance of UHPC is approximately 54% higher than the abrasion resistance of HPC, with UHPC having a 65% higher compressive strength. The surface layer of concrete has a lower wear resistance than the inner layers, which may result from the wall effect during casting. The material mix is different on the surface of the cast part because only a small portion of the aggregate can reach the mold surface. The abrasion resistance of concrete is directly related to the hardness of the material. Therefore, adding hard steel fibers to the concrete raises its abrasion resistance.[56]

Fire resistance

During fire tryouts UHPC tended to early spalling of the heated surface. The reason for this phenomenon is the extremely low transportability of moisture within the tight cement stone matrix. Starting at a temperature of 105°C, free water in the matrix vaporizes, partly diffuses in colder areas of the concrete and condenses there. These colder areas become filled with water and diffusion is not possible anymore. Hence, steam pressure rises. When pressure increases above the tensile strength, an explosive spalling occurs.[57] This process is illustrated in Figure 2.12.

In order to prevent concrete from spalling, polypropylene (pp) fibers can be used. The pp fibers melt above 165°C and their volume expands during and after melting. This increasing volume brings high pressure to the occupied area and creates microcracks. These microcracks advance pore connectivity of the concrete matrix, allowing the vapor pressure to be released without spalling of the surface. This

[55] cf. Fehling, E., et al. (2013), p.148

[56] cf. Zhao, S., et al. (2016)

[57] cf. Smidt, M., et al. (2007), p. 72

countermeasure against explosive spalling can be triggered with an addition of roughly 0.1 to 0.2 vol. % of pp fibers.[58]

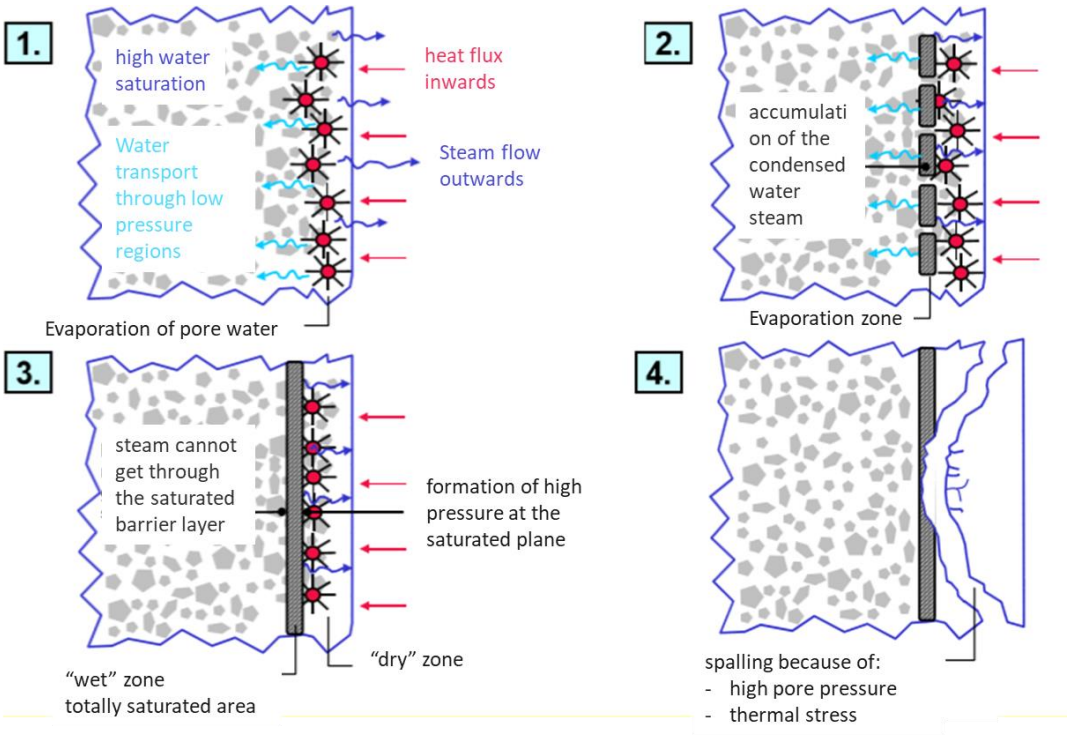

Figure 2.12: Illustration of the development of spalling with UHPC[57]

2.2.5 Known applications of UHPC in sheet metal forming

In literature, there are a couple of approaches to integrate UHPC in the mechanical engineering field. The following segment describes three of them in more detail.

[58] cf. Bamonte, P. and Gambarova, P. (2014), p. 58-59

Ultra-high performance concrete dies for hydroforming[59]

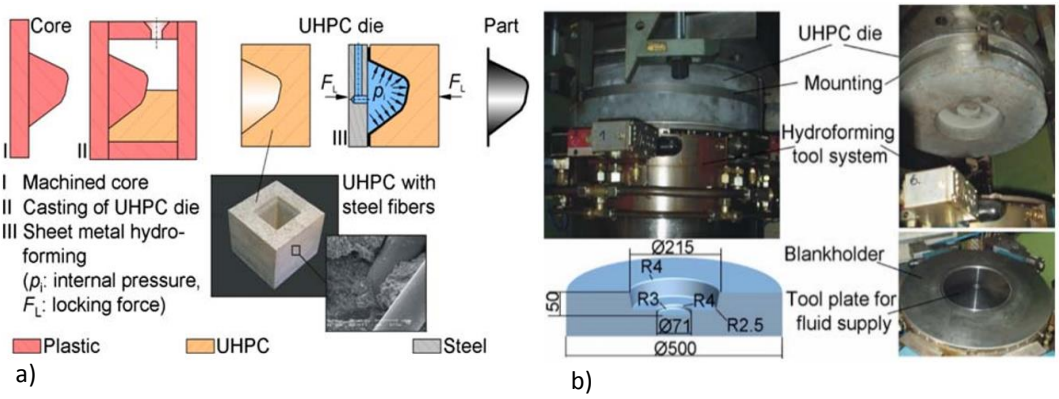

Figure 2.13: Hydroforming die: a) Casting process scheme and b) the hydroforming tool

In this case, UHPC is used for a die in a hydroforming process of DC04 sheets. A rough description of the steps of the experiment is shown in Figure 2.13. The UHPC die is cast in an Ureol mold and tested in the hydroforming tool after a heat curing (not shown in the picture).

The developed UHPC had a compressive strength of approximately 250 N/mm^2 and a Young's modulus of 50,000 N/mm^2. They formed 30 sheets with a pressure of up to 40 N/mm^2 which the concrete endured. In further tests the pressure was increased incrementally with no noticeable effect up to 80 N/mm^2. By further increasing the pressure, the part started to crack at the bottom in the smallest radius. When increasing the pressure to 96.5 N/mm^2 the fractures were getting so big that it started to leak.

Hydraulic concrete as a deep-drawing tool of sheet steel[60]

In this experiment it was investigated, if a high performance concrete coated with a resin could be used in prototyping or even small series production in the automotive

[59] cf. Kleiner, M., et al. (2008), p. 201–208

[60] cf. Schwartzentruber, A., et al. (1999), p. 267-271

industry. The motivation of this experiment was the low cost of the concrete, only 100 $/m^3 instead of 800$/m^3 for the commonly used PRC (polymer resin concrete). Both the die and the punch were made of concrete and tested on a deep drawing line. In Figure 2.14 the investigated parts are shown and in Figure 2.15 the good bond between the concrete and the coating is illustrated.

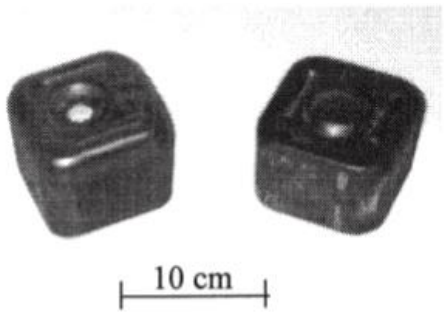

Figure 2.14: HPC resin-coated die and punch

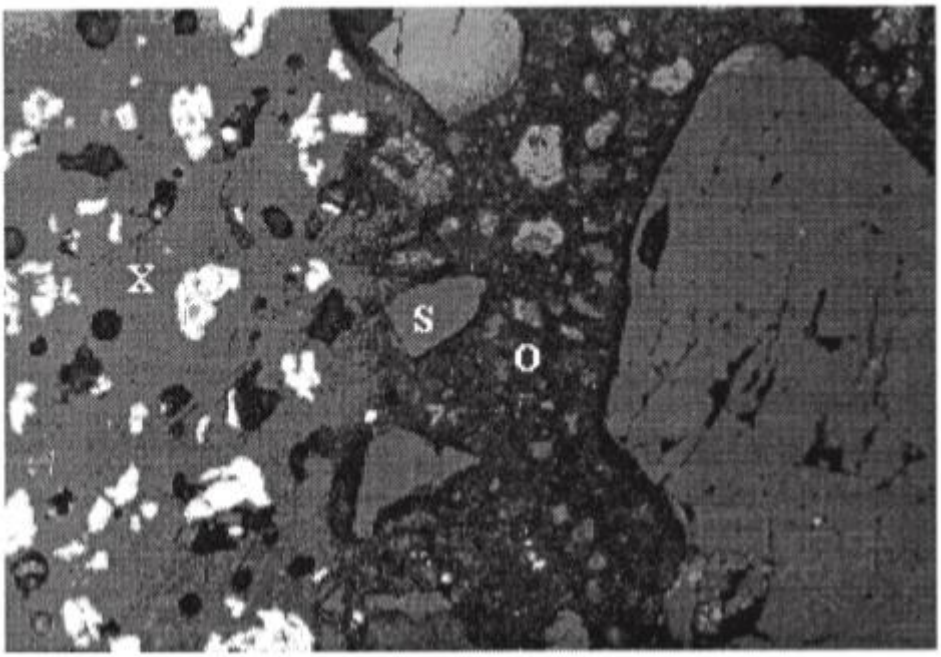

Figure 2.15: Layers of the die and punch, X: gel coat, S: sand, O: HPC

The conclusion of this experiment was the possibility to produce at least 16,000 parts before the gel coat starts to break.

North American Patent: US 2013/0183463 A1[61]

The Spanish company Rovalma S.A. sumbitted the patent "Method for producing highly mechanically demanded pieces and specially tools from low cost ceramics or polymers" in 2013 to the United States Patent Office. In this patent, the company described a concrete deep drawing tool. The geometry and the basic components of the tool are shown in Figure 2.16.

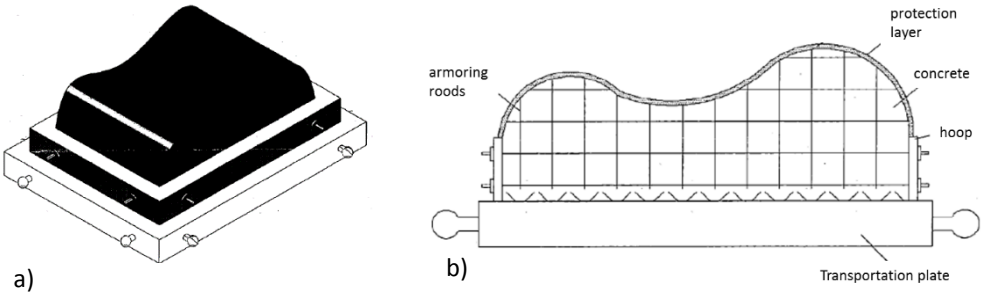

Figure 2.16: Patented tool drawings: a) 3D drawing of the tool and b) section through the middle of the 3D drawing showing all the elements

The requirements for a deep drawing tool are:

- High dimensional accuracy and stability
- good surface condition
- wear resistance
- high mechanical resistance and toughness

These properties are necessary to guarantee the stability of the designed deep drawing process.

The basic concept of this invention is to create a tool using a low cost material, e. g. UHPC, and then coat it with a high value material, e.g. hot or cold sprayed metal, technical ceramic or intermetallic compound, which provides the necessary properties to fulfill the before mentioned requirements.

[61] cf. US patent office (2013)

2.3 Wear in the deep drawing process

In the Oxford English dictionary wear is defined as, “Undergo damage, erosion, or destruction as a result of friction or use”.[62] In other words, wear results from the loss and or the transport of material within a surface.[63] Friction between two moving surfaces is the most common reason for wear. In Figure 2.17 different types of wear are depicted based on different tribological loads.

The wear rate of a material is dependent on the following parameters:[64,65]

- contact pressure
- load velocity
- material of work piece
- coating of the material
- temperature of the material
- chemical reactivity of the material
- roughness of the surface
- lubrication

[62] oxforddictionaries.com

[63] cf. Hutchings, I.M. (2005), p.1

[64] cf. Kato, K. (2005), p. 9-11

[65] cf. Holmberg, K. and Matthews, A. (2005), p.128

Elements of System Structure 1... Base body 2... Opposing body 3... Intermediate medium	Tribological load		Type of wear	Examples	Effective wear mechanisms ● Prevalent ○ Secondarily			
					Ad-hesion	Abra-sion	Surface Spalling	Tribo-chemical wear
2 ... Solid body 3 ... Intermediate (fluid) 1 ... Solid body	Sliding Rolling		Sliding wear Rolling wear	Sliding bearing, rolling bearing, gears, cam shafts	(○)	(○)	●	○
2 ... Solid body 3 ... Intermediate (wear particles, fluid residues, gases or vacuum) 1 ... Solid body	Sliding		Sliding wear	Cylinder liner	●	○	○	●
	Rolling Revolving		Rolling wear	Rolling bearing, gears, cam shafts, wheel/rail	○	○	●	●
	Oscillating		Fretting wear	Fitting surface, bearing seat	●	●	●	●
	Impacting		Impact wear	Valve needle	○	○	●	●
2 ...Particles 1 ... Solid body	Impacting		Two-body abrasion	Impact plate, impact mill	○	●	●	○
	Sliding	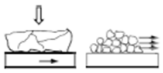		Excavator bucket, rock drill	○	●	○	(○)
2 ... Solid body 3 ... Particles/ loose material 1... Solid body	Sliding		Three-body abrasion	Impurities in bearings and guides	○	●	●	○
	Rolling	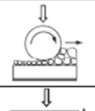		Roller mill	○	●	●	○
	Impacting			Jaw crusher	○	●	●	(○)
2 ... Fluid with particles 1... Solid body	Flowing	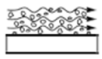	Hydroerosion	Pumps, transmission pipes	(○)	●	●	○
2 ... Gas with particles 1... Solid body	Flowing		Abrasive erosion	Pneumatic conveyor systems	○	●	●	○
	Sliding Impacting	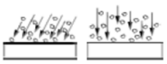	Oblique impact erosion, Impact erosion		○	●	●	○
2 ... Fluid 1... Solid body	Flowing Vibrating	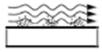	Cavitation erosion	Pumps, valves, water turbines			●	○
	Impacting Sliding		Drop erosion	Rotor blades, steam turbines			●	○
	Flowing	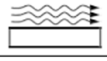	Fluid erosion	Pumps, valves, pipes		(○)	○	●
2 ... Gas 1... Solid body	Flowing	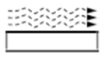	Gas erosion	Gas turbine, thermal shield				●

Figure 2.17: Types of wear[66]

[66]cf. Sommer, K. et al., (2014), p. 15

During the deep drawing process friction appears in (1) the contact area between the blank holder and the drawing ring or the die, on (2) the drawing edge radius area and on (3) the punch radius area; the different areas are shown in Figure 2.18.[67] As mentioned before, friction is a source of wear, therefore those three areas are the critical areas for wear on the deep drawing tool. According to Hoffmann H. et al. the area with the highest wear depth is the drawing edge radius area.

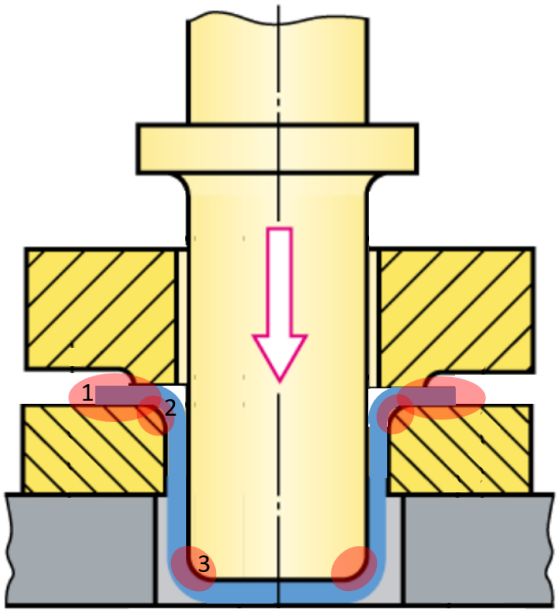

Figure 2.18: Areas of friction in the deep drawing process[68]

The wear of the tool defines the tool life and therefore the possible number of produced parts. The life of a tool ends when the necessary part quality cannot be guaranteed anymore, because of insufficient dimensional accuracy and surface quality of the tool.[69]

[67] cf. Klocke, F. and König, W. (2006), p.333

[68] cf. Dillinger, J. et al. (2007), p. 96

[69] cf. Klocke, F. and König, W. (2006), p.141

2.3.1 Wear mechanisms

Abrasion

Abrasion is scratching and micro-chipping of the base body by the hard peeks on the surface of the opposing body, due to its roughness, or by hard particles in the intermediate.[70] Figure 2.19 depicts the principle of abrasion.

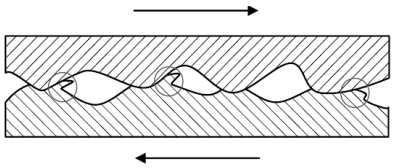

Figure 2.19: Abrasion[71]

In the forming process, the basic body is usually the tool and the opposing body is the work piece. The hard particles, which get pressed into the tool surface, are the hard-phases within the blank material, e.g. carbides of the alloy elements, or contaminants on the surface of the blank.[72]

Adhesion

Adhesion is the formation and separation of atomic connections (micro wear) between the basic and the opposing body.[70] In Figure 2.20 the principle of adhesion is depicted.

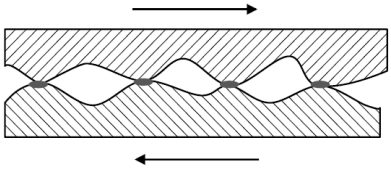

Figure 2.20: Adhesion[71]

[70] cf. Habig, K.-H. and Woydt, M. (2014), p.E90

[71] Klocke, F. and König, W. (2006), p.142

[72] cf. Klocke, F. and König, W. (2006), p.142

This wear mechanism expresses itself by the movement of material from the softer to the harder friction partner and occurs because of the high surface pressure between them. In the case of deep drawing, material from the softer blank gets transported onto the surface of the harder tool.[73]

Surface spalling

Surface spalling is a result of the changing stress in the surfaces of the basic and the opposing body. Hence, cracks and further severing of particles occur[70], shown in Figure 2.21.

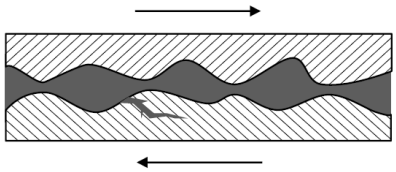

Figure 2.21: Surface spalling[71]

Surface spalling occurs on areas where roughness is high or the tool has remaining grooves and burrs from grinding.[74]

Tribochemical wear

Tribochemical wear exists because of a chemical reaction of one or both of the bodies with components of the lubricant of the ambient medium, due to friction induced chemical activation of the surfaces.[70].

[73] cf. Klocke, F. and König, W. (2006), p.144

[74] cf. Klocke, F. and König, W. (2006), p.146

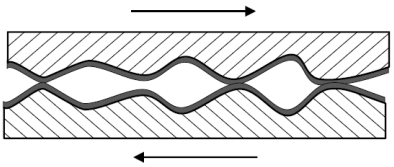

Figure 2.22: Tribochemical wear[71]

The affected areas, shown in Figure 2.22, are changing their chemical composition which results in different properties of the material. Brittle and hard reaction layers are only able to remove limited amounts of tribologically induced stresses and spall of the surface when reaching a critical thickness. The softer reaction products are created continuously and get removed abrasively.[75]

2.3.2 Methods to analyse wear

Premature function loss or failure of a part is a sign of the actual stress being higher than the part was designed for. The reasons for this can be unsuitable materials or a deviation in shape. In order to analyse the wear of the part a structure and stress analysis needs to be done. Those analyses most of the time lead to a target-actual comparison.[76]

Structure analysis[77]

The main goal of the structure analysis is to find the cause of damage. All of the involved components need to be investigated, because different wear marks can occur on different work pieces.

[75] cf. Klocke, F. and König, W. (2006), p.147

[76] cf. Sommer, K. et al., (2014), p. 35

[77] cf. Sommer, K. et al., (2014), p. 37-38

The changes in macro geometry of the damaged parts can be obtained with the following measurement methods and instruments:

- mechanical and optical scanning measurement methods
- light microscope and scanning electron microscope
- making imprints of the surface for further investigations under a microscope

To get further knowledge an additional investigation of the boundary layers of the structure needs to be done by means of metallographic sections, hardness test and residual stress measurements.

Stress analysis[78]

Stress analysis targets the determination of the stresses in the boundary layer of the tribological contact. In this analysis the term “stress” stands for external impacts like forces, moments, movements and temperatures.

This analysis is supported by the operational records of the production machine, the finite element simulation software and other supporting software.

[78] cf. Sommer, K. et al., (2014), p. 38-39

3 Experiment procedure

The experiment can be roughly divided into three major steps. First the production of the concrete punch, then deep drawing tests and finally measuring of the punch and the formed blanks.

3.1 Production of the concrete punch

With the exception of the mold production each step of this part of the experiment was done at the LKI.

Figure 3.1: Cup geometry punch in steel and UHPC

3.1.1 Production of the mold

For this experiment, a tool with a cup geometry was chosen. As usual in casting, the first step was creating a CAD drawing of the casting mold for the concrete punch (punch shown in Figure 3.1). Additionally to the mold a fixture (Figure 3.3) was needed to connect the punch to the deep drawing tool. The fixture consists of a flange, where the punch and the tool are connected with eight screws, and three threaded rods for reinforcing the concrete and also to guarantee a connection between the flange and the concrete. To be able to demold the punch without

damaging the form, the form had to be divided into two parts. The mold material used was a plastic based on PU, made by the RAMPF Holding GmbH & Co. KG. The Raku-Tool® WB 1404 was chosen based on the known manufacturability, especially the good polishability[79], and the lack of chemical reactions with UHPC. The mold was produced in the workshop of the research group Tools and Forming; the milling of the mold is shown in Figure 3.2.

Figure 3.2: Milling of the casting mold

[79] cf. rampf-gruppe.de

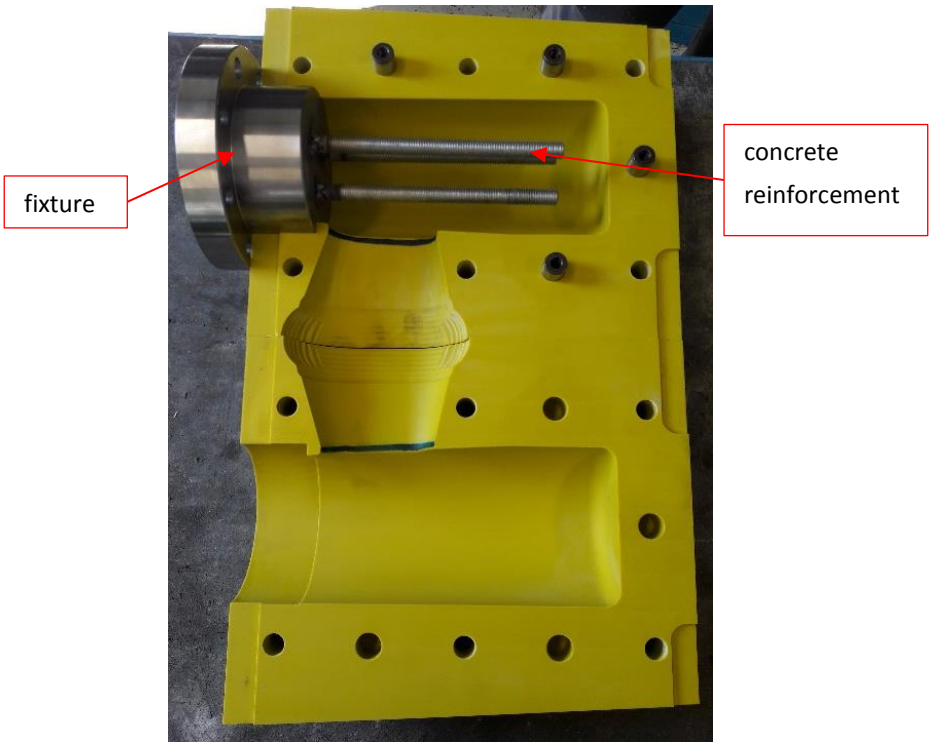

Figure 3.3: Mold with fixture

3.1.2 Casting of the punch

The casting of the punch was done at the Laboratory for Structural Engineering (LKI) of the Graz University of Technology. Due to a non-disclosure agreement with the laboratory it is not possible to explain the exact mixing procedure or the exact recipe of the UHPC, but a rough description can be given:

1. Mixing of the dry components
2. Addition of the liquid components
3. Mixing for a certain time
4. Addition of the steel fibers

Table 3.1 lists the materials used to mix the ultra-high-performance concrete used in this thesis.

Table 3.1: Components of the UHPC

Cement	**CEM I 52,5 N C_3A-free**
Micro-silica	„RW Füller“, Fa. RW Silizium
Quartz flour	„Dorsilit 16900“, Fa. Dorfner
Additives	Superplasticizer (Prement 500)
	De-foaming agent (Prement 500)
Steel fiber	9/0.115 mm structured

Before the concrete is put into the mold, its spread flow has to be tested. Therefore, a so-called Hängermann-cone according to EN 1015-3 is put on a glass plate, filled with concrete, lifted up and then the time until it expands to a 200-mm circle as well as the maximum spread diameter (mean value of 2 diameters) is measured. The concrete needs to flow until a circle with a minimum diameter of 250 mm is filled and should have a flow time under 7 seconds. If all the requirements are met the UHPC can be cast and vibrated afterwards, to facilitate easier evacuation of air bubbles. Before the concrete is put away to dry, water needs to be sprayed on the surfaces which are not covered by a wall of the mold, e.g. the filling hole of the punch mold. Additionally to the water, a plastic foil is put on the open surfaces to keep these areas from curing quicker than the rest of the cast part.

Pictures of the casting process are displayed in Figure 3.4.

a) b)

c) d)

Figure 3.4: Steps of the casting process: a) Mixing machine, b) spread flow test, c) filling of the mold, d) vibrating to reduce the air in the concrete

Release agent testing

The results of the first casting of the punch were not sufficient (Figure 3.9- cavities on the surface of the punch). Therefore, in addition to changes in the concrete mix, the veracity of the release agent was also subject of an investigation. Three possible release agents were tested.

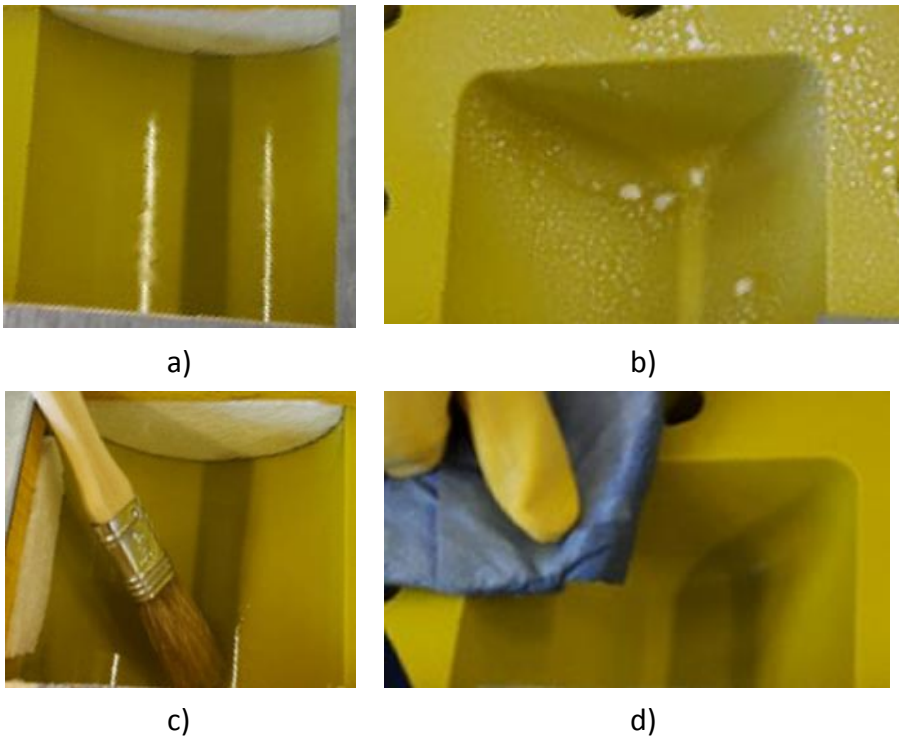

Figure 3.5: Applying of the different release agents: a) brake fluid, b) sprayed release agent, c) release agent applied with brush and d) release agent applied with cloth

The possible release agents were the previously used release agent, brake fluid and a sprayable release agent. The brake fluid is not a certified release agent, but it was chosen because it is known to wet a plastic mold almost totally in contrast to the other release agents. The previously used release agent was applied with a brush and a piece of cloth, to investigate the dependence of the agent's performance on different application options. When applying the agent with a brush more fluid stays on the surface of the mold than applying with a piece of cloth.

The results of this investigation are depicted in Figure 3.6. Even though the sprayed release agent and the brake fluid did not cause any cavities, the surface quality was not as high as the surface quality resulting from the previously used release agent applied, with a piece of cloth. Therefore, the originally selected release agent (applied as a very thin film with a cloth) was used in the casting of the final concrete punch.

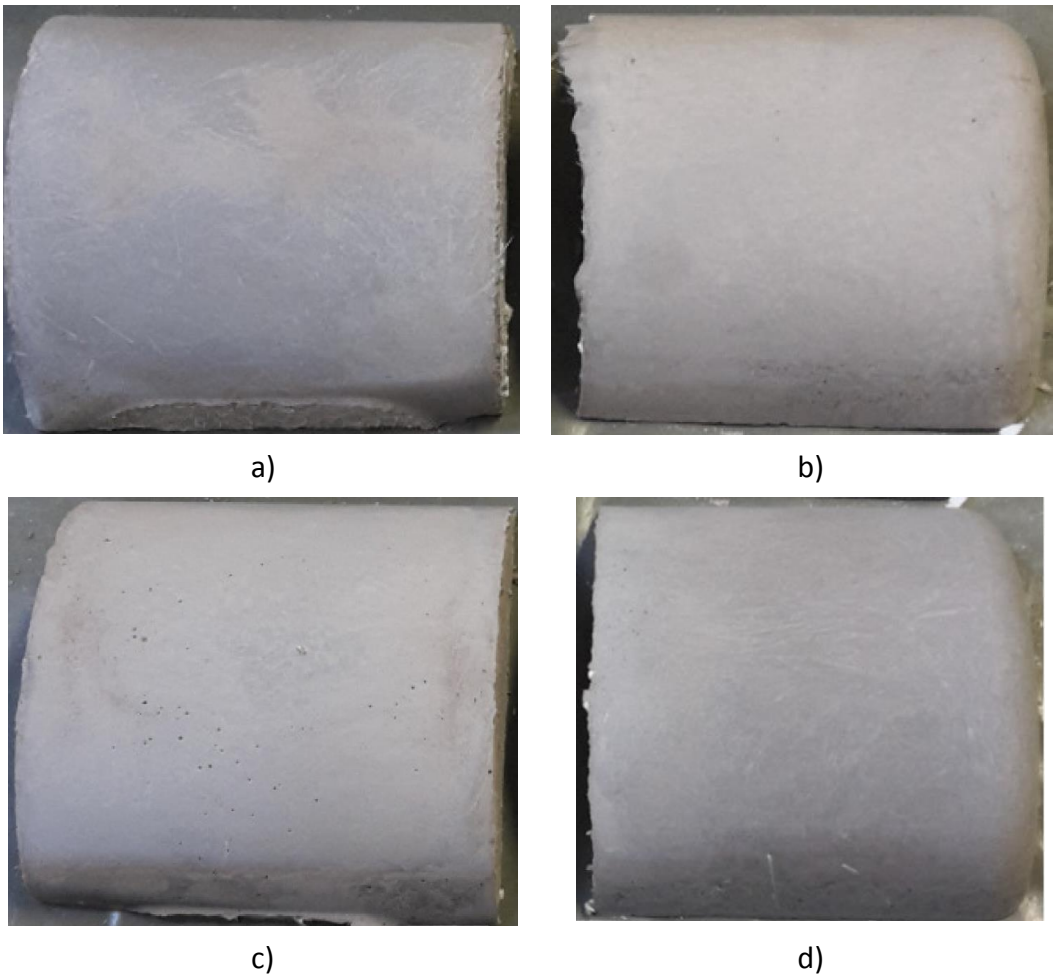

Figure 3.6: Results of the release agent tests: a) brake fluid, b) sprayed release agent, c) release agent applied with brush and d) release agent applied with cloth

3.1.3 Curing of the concrete

According to experts of the Institute of Technology and Testing of Construction Materials at the Graz University of Technology, the concrete hardens depending on its composition with a time depending function. Reference values of 28 day old concrete are taken, according to construction standards. UHPC without heat treatment increases its strength after 28 days remarkably, an increase of approximately 20% can be expected to an age of 2-3 months. In nature strength increases further over years. If appropriate heat curing is applied a 56 day strength is reached after approximately one week. Therefore, heat treatment for the concrete punch was chosen to be done.

A very strict schedule had to be upheld:

- concrete needs to be demolded 24 hours after the casting
- curing has to start shortly after the demolding
- climate chamber with the concrete punch in it needs to be set for 90% humidity with a slow rise of the temperature from room temperature to 90°C (increase of 10°C every hour)
- after reaching target temperature of 90°C, both temperature and humidity stay as set for 48 hours curing time
- cool down to room temperature has to happen at the same speed as heating up

After the heat treatment (including slow cooldown), the cast part is finished.

3.1.4 Testing of the concrete

In order to find out the Young's Modulus and the compressive strength of the mixed concrete, small test blocks (40x40x160 mm) were produced using the same concrete mix as the punch. Those test blocks were also subjected to the same curing process as the punch. In Figure 3.7 the test set up at the LKI is depicted.

To start the tests for the concrete's Young's Modulus it is necessary to either obtain the compressions strength beforehand or use known values of the material. With compression strength values a preload (10% of the maximal load) and a maximum load are calculated. The test machine stresses the test block first with the preload, then the load gets raised to the maximum load. This load level is held for 60 seconds and then reduced to the preload level. This procedure is repeated three times, to obtain the calculation values of the Young's modulus at the 4^{th} passthrough. At the end of these tests, one more test run is done, at which the compression strength value is obtained and the test block gets destroyed.

a) b)

Figure 3.7: Young's Modulus Test of the UHPC: a) before the test and b) after the test

3.1.5 Properties of the cast concrete

In this study two different concrete punches were produced. Punch 1, made of concrete mix 1, was used in the preliminary tests and Punch 2, made of concrete mix 2, was used in the main deep drawing tests. This was due to the fact that the casting of the first concrete mix resulted in a scrap part. The first punch had a big number of huge cavities, hence the recipe of the concrete was reevaluated and the changes are listed in Table 3.2.

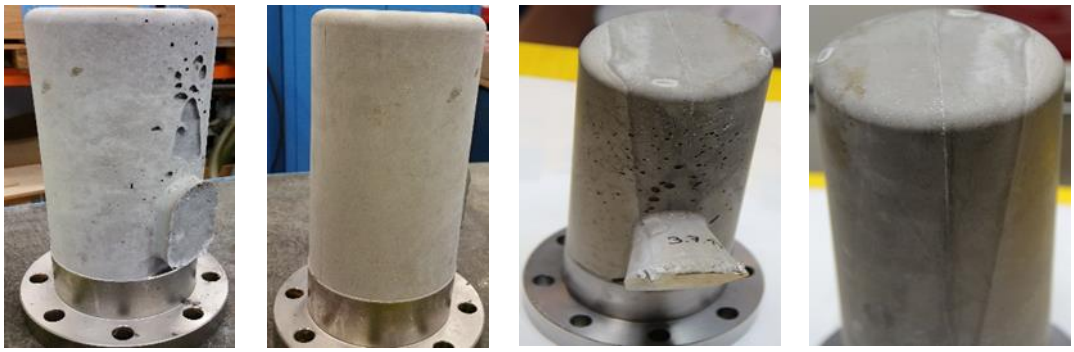

a) b) c) d)

Figure 3.8: Punches after the curing: a) Punch 1 front, b) Punch 1 back, c) Punch 2 front and d) Pinch 2 back

Table 3.2: Differences between the two concrete mixes

Property	Concrete Mix 1	Concrete Mix 2
Amount of steel fibers [%]	1.34	0.67
W/C value	0.25	0.27
Spread flow [mm]	256	260
Young's Modulus [N/mm^2]	50,590	51,169
Compressive strength [N/mm^2]	187	205
Curing condition	climatic chamber	in water in the heating chamber*

*the climate chamber was not available at the needed time to cure the punch correctly

3.2 Deep drawing tests

The deep drawing tests were conducted with a 400t hydraulic press from Schuler located at the research group Tools and Forming.

3.2.1 Preliminary tests

In order to make an efficient DoE preliminary tests of the concrete punch were necessary. The goal of these tests was to find out if the punch was able to withstand the forces created during the deep drawing process. Unfortunately, the first casting of the punch resulted in a scrap part, shown in Figure 3.9. This situation was also fortunate, because it opened up the possibility of performing the preliminary test without considering the consequences of damaging the punch for the real test.

a) b)

Figure 3.9: Punch 1: a) side with huge cavities and b) area with no cavities

Given the fact that the huge cavities were only located on one side of the punch, the assumptions made by the results of the preliminary tests were valid for the further inspection of the punch in the main tests. Because one side of the punch was without cavities, therefore the behavior of this side must be the equal to the behavior of the following cast punch.

It was decided to slowly increase the strength of the blanks used for the deep drawing, starting with aluminum blanks, moving on to the DC04 steel blanks and finally trying out the hard TPN 780 steel blanks. The parameters of the deep drawing process were chosen to obtain a cracked scrap part, to have the maximum impact on the punch. The exact parameters are shown in Table 3.3.

Table 3.3: Parameters for the preliminary tests

Part number	Blank material and thickness [mm]	Distance [mm]	Press force [kN]	Drawing velocity [mm/s]	Blank holder force [kN]	Drawing depth [mm]
1	**Alu 5xxx 1mm**	0	1000	30	160	55
2	**Alu 5xxx 1mm**	1.6	1000	30	160	55
3	**DC04 1.5mm**	1.6	1000	30	160	55
4	**DC04 1.5mm**	0	1000	30	160	55
5	**TPN 780 1.5mm**	1.6	1000	30	160	55
6	**TPN 780 1.5mm**	0	1000	30	160	55
7	**DC04 1.5mm**	1.6	1000	20	160	35*
8	**DC04 1.5mm**	1.6	1000	20	160	50

* blank did not crack

A distance of 1.6 mm between blank holder and drawing ring was tested in order to see if the applied minimum blank holder force of the press influenced the condition of the formed blank. With this distance, the blank could slide better over the drawing ring.

The preliminary tests were stopped after these eight tryouts because the defective side of the punch was getting worse and the steel fibers, pointing out of the surface, were clinging to the blank and the concrete was crumbling away. The other side of the punch, without huge cavities, did not show any visible changes of the surface condition. Therefore, it was concluded that the concrete could be tested further, just not with an advanced high strength steel, but with the softer DC04.

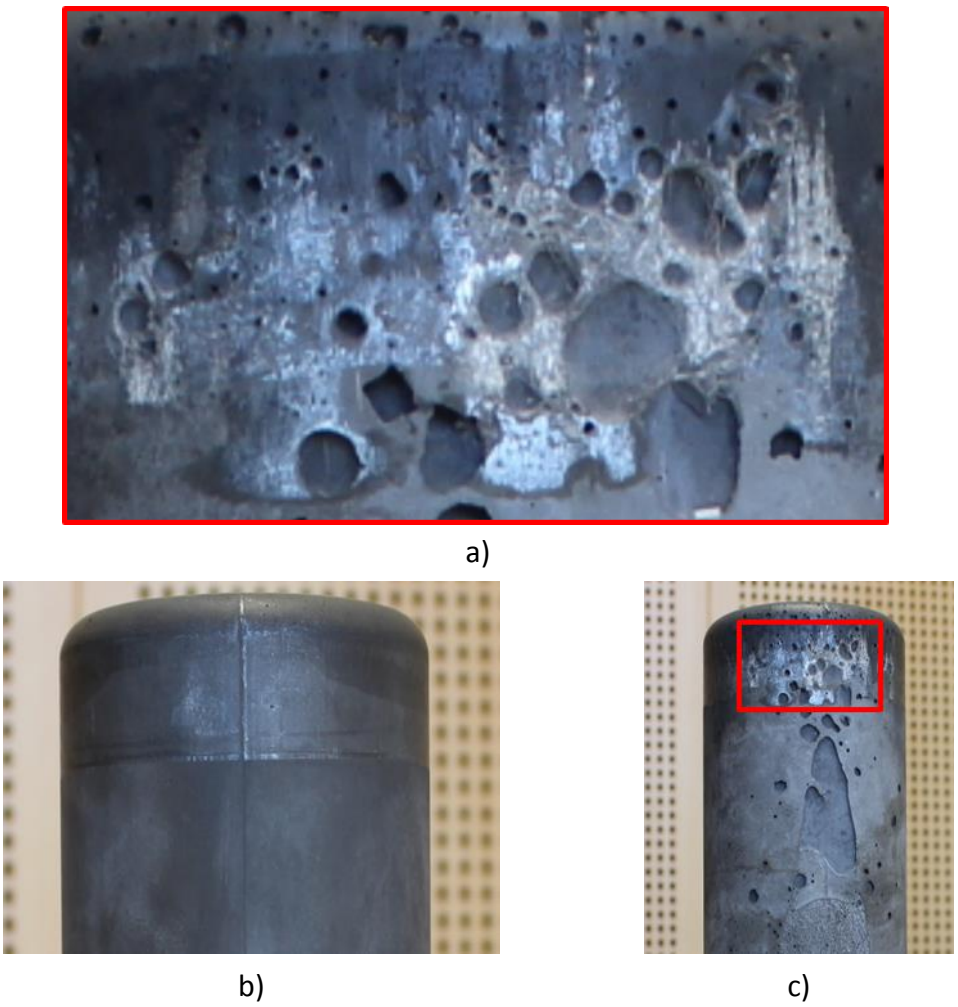

Figure 3.10: Punch after preliminary tests: a) zoom of marked area in c), b) side without cavities and c) side with cavities

One very interesting outcome of the preliminary test was abrasion of the aluminum on the punch; the shining aluminum parts are visible in Figure 3.10.

3.2.2 Design of experiment

The experiment was done with the same material, DC04 1.5 mm thick; the same lubricant, Wisura FOM 5010; the same press force, 800 kN; and the same blank holder force, 160 kN. The parameters that were variated are listed in Table 3.4. In Figure 3.11 all the formed blanks from the main tryouts are depicted.

Figure 3.11: The deep drawn blanks from the main tests

Table 3.4: Parameters for the deep drawing tests

Number of pieces	Drawing velocity [mm/s]	Drawing depth [mm]	Blank numbers
50	20	35	0.1 – 5.10
50	50	35	6.1 – 9.10; 15.1–15.10
50	100	35	10.1 – 14.10
50	150	35	16.1 – 20.10
50	150	40	21.1 – 25.10

To allocate the imprints on the blanks to the UHPC punch or to the behavior of the blanks, additional tests with a steel punch were made for each variation of parameters.

Lubrication

After each punch stroke, an indetermined amount of lubricant remained on the punch, which results in different lubrication levels for the first blanks. In order to eliminate this variable, the punch was lubricated before the deep drawing tests started.

The Wisura FMO 5010 from the Fuchs Wisura GmbH is a chlorine- and heavy metal-free forming lubricant. This lubricant is mainly used with ferritic structures and sheets with a thickness of up to 12 mm. The lubricant is to be used undiluted.[80] In Table 3.5 the properties of the Wisura FMO 5010 are listed.

Table 3.5: Properties of the lubricant[80]

Properties	Unit	Value	Examination under
Density at 15°C	g/ml	0.948	DIN 51 757
Viscosity at 40°c	mm^2/s	175	DIN 51 562
Flashpoint	°C	>200	DIN 51 376

Blank material - DC04

DC04 is a high strength deep drawing steel commonly used in the automotive industry. The chemical composition and mechanical properties are shown in Table 3.6.

[80] cf. feintool.com

Table 3.6: Characteristics of DC04[81]

C [%]	Mn [%]	P [%]	S [%]	$R_{p\ 0,2}$ [MPA]	R_m [MPa]	A_{80} [%]	$r_{90/20}$	$n_{10\text{-}20/Ag}$
0.08	0.04	0.03	0.03	140-210	270-350	38	1.6	0.18

3.2.3 On-site tests

The project partner, MAGNA Cosma Engineering Europe GmbH, has the facilities to test materials with a much higher number of blanks. This machine was constructed for a specific geometry, namely the interchangeable inserts, of the test object, therefore the cup punch cannot be tested in this machine. Hence, the interchangeable inserts (Figure 3.12) were cast with the same concrete mix as the punch.

During these tests, the metal sheets are slid partly over the rounded edge of the insert and then the sheets is bent by 90° (movement marked in Figure 3.12 with a red arrow). The tests end either when the concrete breaks or it endured 1000 bends. After the tests, the concrete insert is investigated with an Alicona Imaging GmbH measurement system to see the resulting wear of the material.

The results of this investigation are still pending.

[81] thyssenkrupp.at

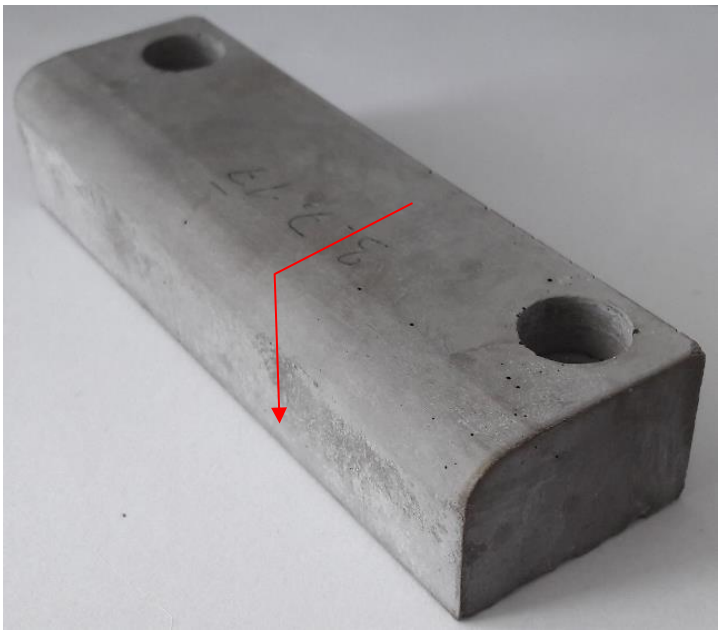

Figure 3.12: Interchangeable insert

3.3 Evaluation of the punch and the formed blanks

For evaluating the punch abrasion and furthermore the influence of the punch's roughness and abrasions on the formed blanks, different optical measurement systems were used. The concrete punch was measured before and after the deep drawing tests with the ATOS III 3D scanning system from GOM GmbH. The inner surfaces of the formed blanks were compared with blanks formed with a steel punch, using the same process parameters as with the concrete punch, under a light microscope from Nikon. Both optical measurement systems were available at the research group Tools and Forming.

3.3.1 Inspection of the punch with a 3D scanner

The surface investigation of concrete is not a topic that is well studied, therefore some ideas were tested in preliminary tryouts. Similar to the preliminary tryouts for the deep drawing tests, the search for the best surface measurement system was also done with the first cast concrete punch.

Preliminary tryouts

The main objective of these tryouts was to find the best way to produce a 3D image of the punch in as accurate as possible quality.

The first idea was to investigate the surface with an optical measurement system by the Alicona Imaging GmbH. After consulting the FELMI (Institute of Electron Microscopy and Nanoanalysis) at the TU Graz and employees of the Alicona Imaging GmbH, it became clear the punch was too large and too heavy for their systems. Because the punch needed to also be measured before the deep drawing tests, cutting it in pieces was not an option. For this reason, making imprints of the punch was suggested. This idea was tried out in two different ways.

The first test used a cold-curing resin for surface testing and impressions produced by the Heraeus Kulzer GmbH. The composite was mixed together as instructed and applied to the punch (Figure 3.13a). The removal of the resin was not easy and did not happen without harming the surface of the concrete punch. Figure 3.13b illustrates the traces of concrete, which were removed from the punch and kept clinging to the resin. The goal of the tryouts was to find a way that did not harm the surface of the punch, therefore, this resin was eliminated from consideration.

a) b)

Figure 3.13: Imprint tryout with the cold-curing resin: a) resin applied on the punch and b) resin removed from the punch

The next attempt to fabricate a usable imprint of the punch's surface was done by an employee of the Alicona Imaging GmbH. He applied a two component plastic to the punch, which is commonly used by the company. The usual curing time of the paste is 15 minutes, because of the bigger amount applied it was decided to let it dry for an hour. Even with a longer curing time it did not fully harden and the paste was still liquid on the surface of the punch. The traces left by the plastic are visible in Figure 3.14a. A second attempt with a curing time of a whole day, results were not positive. Figure 3.14 displays the second failed try. Since the radius area of the punch was replicated to a tolerable amount, the Alicona Imaging GmbH tried to investigate it with one of their measurement system. Even though their systems are state of the art, they were not able to produce a usable image of the imprint.

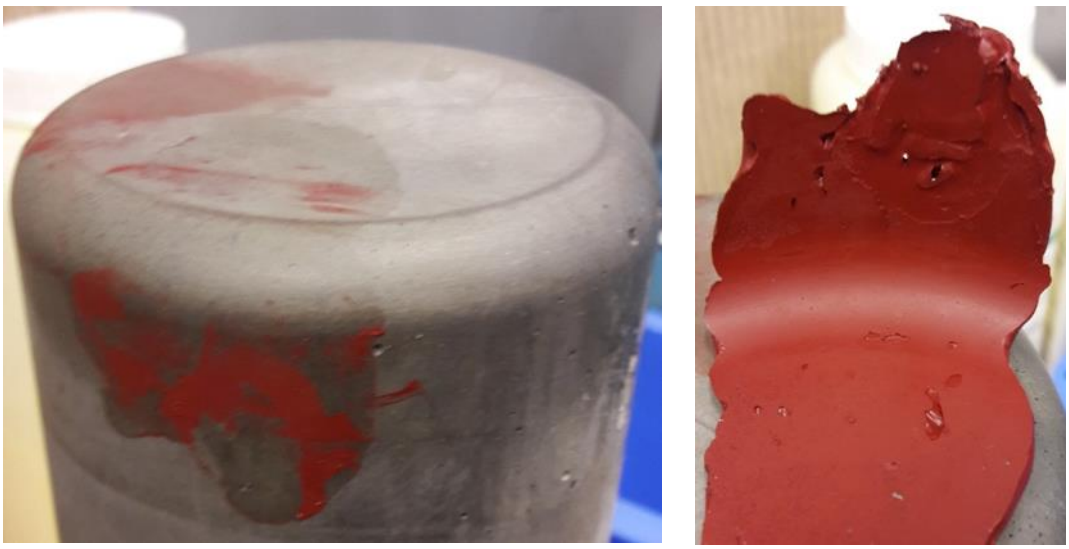

a) b)

Figure 3.14: Tryout with Alicona Imaging GmbH: a) punch after both attempts and b) imprint created at the second try

The last system to try was the 3D measurement system Atos III by the GOM GmbH. This system could produce a usable 3D image of the punch and was therefore chosen for the main investigation of the concrete punch. The exact procedure of how to carry out this process is described in the following paragraphs.

Main investigation

The ATOS III system scans the real object and generates a digital 3D surface of it, which can be compared to the CAD drawing of the part.

The technical specifications of the scanner are shown in Table 3.7.

Table 3.7: Technical specifications of the ATOS III scanner[82]

Measurement points		4,000,000
Measurement time	sec	2
Measurement area	mm^2	150x150 – 2000x2000
Distance of measurement points	mm	0.07 – 1.0

The scanner (shown in Figure 3.15) has 2 cameras, one pointing to the object from the left side and one from the right, as well as an optical scanner in the middle. Near each camera laser pointers are located, which indicate the correct focusing of the cameras on the object, by moving together to one laser point on the surface of the to be investigated object.

Procedure of the measurement

To make a 3D replica of an object the following steps have to be completed:

1. Preparing the measuring area (Figure 3.15)
    a. the scanner with the correct measuring field (550x550x550 mm in this case) needs to be fixed on the tripod and connected via cables to the computer
    b. the room and the table, where the test object will lie, needs to be as dark as possible

[82] tf.tugraz.at

c. starting the computer with the ATOS software and the scanner

2. Preparing the test object
    a. the object needs to be free of dirt and fingerprints
    b. the reference points (with a diameter of 5 mm, in this case) should be distributed on the object, so that from each side at least four points can be seen by one camera and also not put on the critical surface (in this case the radius area of the punch)
    c. it is necessary to apply a white 3D spray on the surface of the object, to minimize its reflection
    d. the reference points need to be cleaned from the 3D spray
    e. because of the white spray, it is not recommended to apply the spray on the test object at the measuring area, so the object needs to be put on the table of the measuring area as carefully as possible

Figure 3.15: Test set up of the ATOS III 3D scanning system

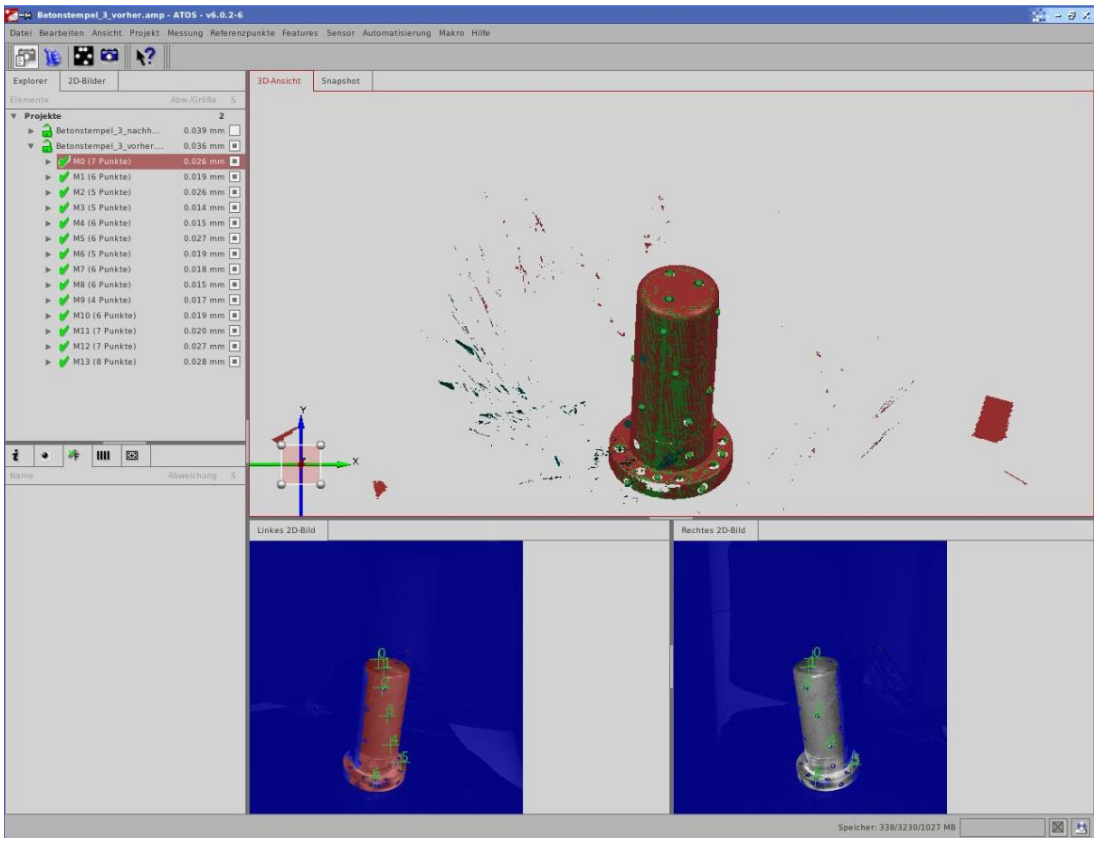

Figure 3.16: Screenshot of the ATOS software

Before the measuring can be started the scanner needs to be calibrated to the decided measuring field.

Now the prepared part needs to be located within range of the scanner, which can be verified by the live picture provided on the computer screen (Figure 3.16). This live picture also shows how many reference points the scanner recognizes and also if the lighting, which can be regulated within the software, is correct. With the reference points the software creates many 3D surface objects of the part which it puts together into one object by referring each measurement to the other. Obviously the scanner cannot predict the surface condition behind the reference points, but it automatically closes those holes while polygonising the measurements. This is why, it is not recommended to put the reference points onto the critical surfaces, because the closed holes of the points do not represent the correct surface condition under the reference points. This can lead to crucial variants in the results of the measurement. This created net of the object can be compared to the actual geometry of the CAD drawing in the GOM Inspect software.

3.3.2 Inspection of the formed blanks with a light microscope

The focus of this thesis is the investigation of the concrete punch, but to be able to make a profound statement about the reliability of the deep drawing process, the effects of the concrete punch's wear on the blanks need to also be investigated. Therefore, the radius area of the formed blanks' inner surface is inspected for deformations with a light microscope.

The test set up of the inspection of the formed blanks is shown in Figure 3.17.

Figure 3.17: Used light microscope

Procedure of the measurement

Even though the formed blanks fit under the light microscope, they needed to be cut slightly above the radius surface so only the bottom surface and the radius are left. (Figure 3.19: a) formed blank and b) cut specimen). After cleaning the tailored specimens, the areas to be investigated were marked and numbered. The area number 1 and 3 are always located on the mark of the separating joint from the punch, then areas 2 and 4 are located 90 ° to area 1 and 3.

Because of the bended radius area the lightning of the specimen was very difficult and did not always result in a perfect picture (an example is shown in Figure 3.18). In

the software for the light microscope it was possible to measure the sizes of the marks made by the punch and to also add a scale into the picture (Figure 3.18). The resulting figures were exported as a portable network graphics (.png) file.

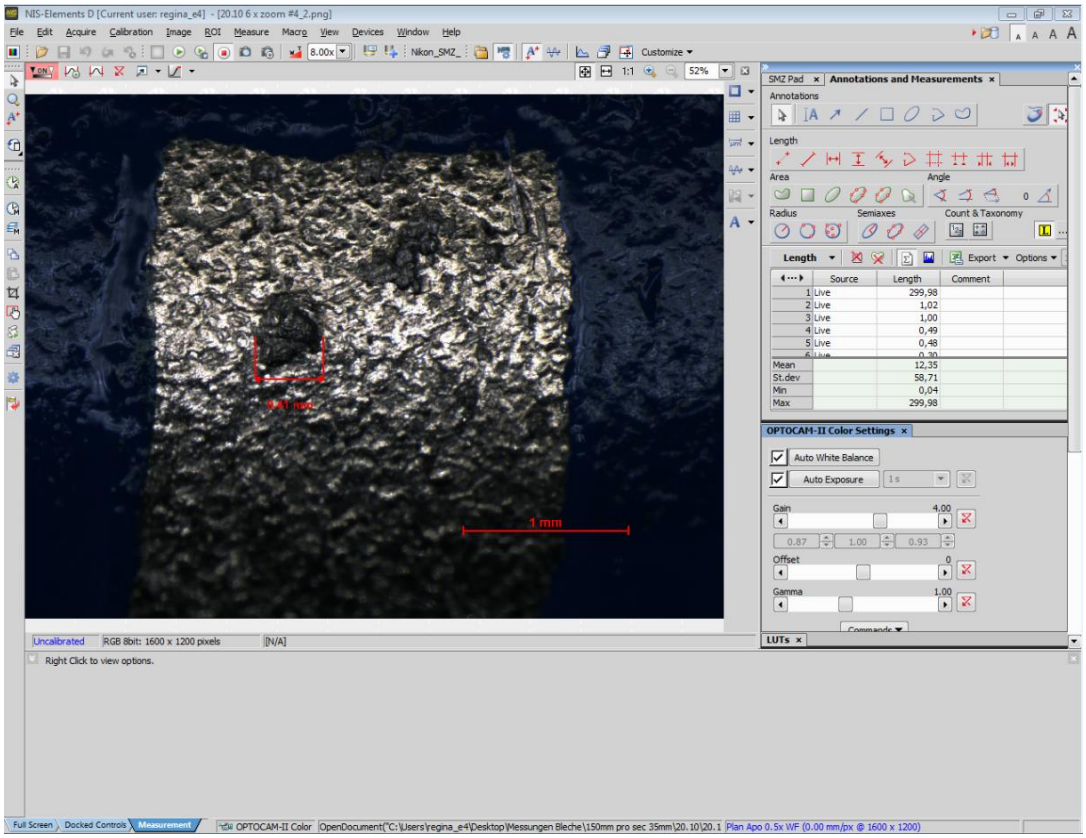

Figure 3.18: Screenshot of the software for the light microscope

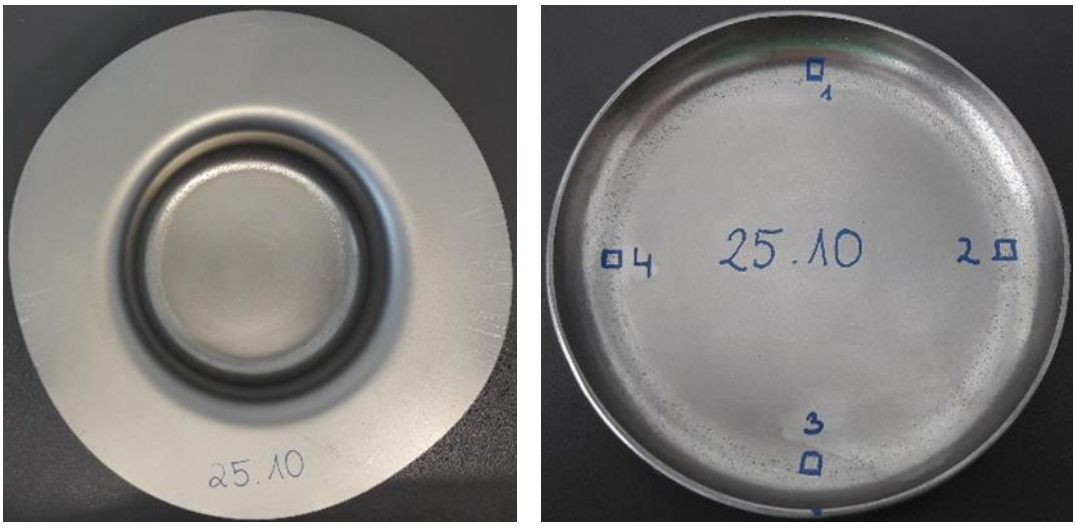

a) b)

Figure 3.19: a) formed blank and b) cut specimen

4 Results

This chapter discusses the outcome of the previously described practical experiment, with the focus being on the radius area of the punch and on the inner side of the blanks, where – as expected – the highest amount of abrasion could be measured.

4.1 Evaluation of the punch

During the deep drawing tests, because of lubrication no abrasion was visible on the punch. After thoroughly cleaning the punch, different levels of abrasion on the radius surface were coming to light; they are depicted in Figure 4.1.

Figure 4.1: Punch after cleaning

As mentioned previously in chapter 3, the punch's surface was measured and compared to the actual geometry, before and after the deep drawing test. The results of this investigation are displayed in the following paragraphs.

In Figure 4.2 it is obvious the punch seems to be slanting to the right, which has happened due to a combination of manufacturing tolerances, the concreta's shrinking and a certain inaccuracy of measurements. The peak and the variance of the dimensional deviation of the left and right radius surface from both measurements are listed in Table 4.1.

Corresponding to the deviation of the variances from Table 4.1, it is possible to point out, while comparing Figure 4.2 and Figure 4.3, that the left side of the punch has been worn off more than the left side. This occurred because of the uneven curing of the punch.

Table 4.1: The geometrical variance of the measured net and the CAD geometry of the punch before and after the deep drawing tests

	Before **left side/right side**	**After** **left side/right side**
Max/Min variance [mm]	-0.27/+0.23	-0.48/-0.22
Mean of the variance [mm]	-0.05/+0.08	-0.22/-0.09

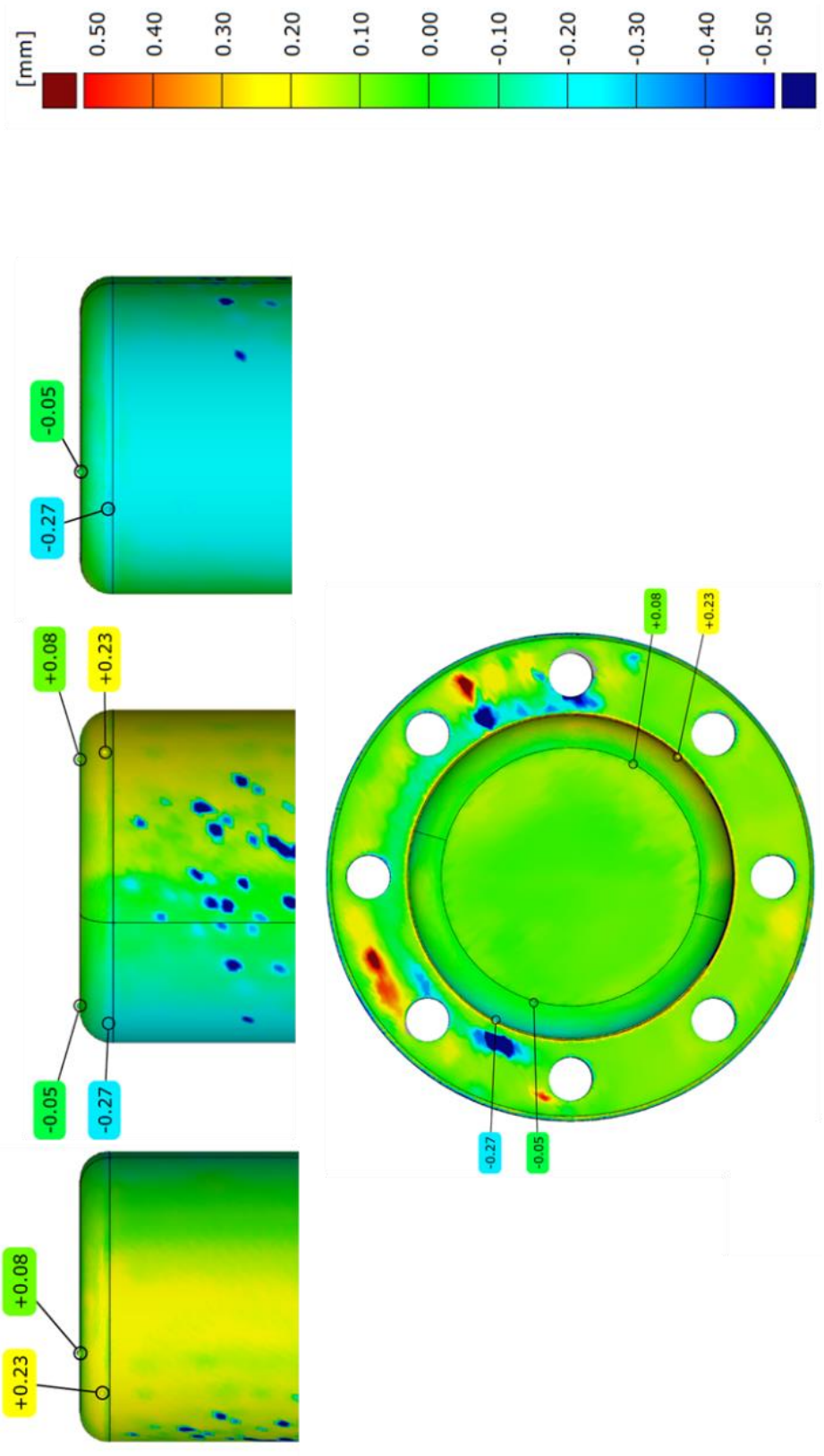

Figure 4.2: Variance between the CAD drawing and the optical measurement of the punch before the deep drawing tests

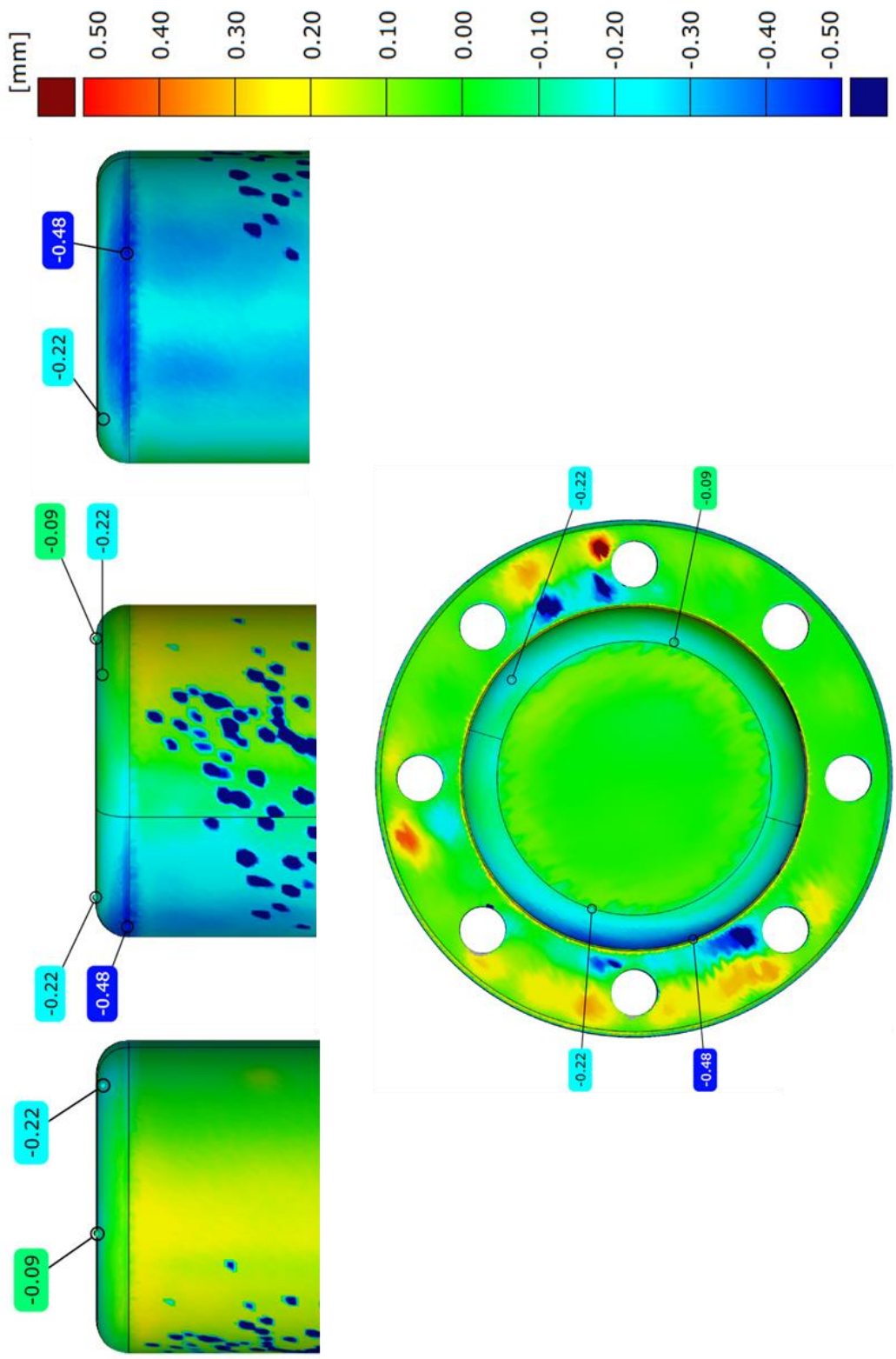

Figure 4.3: Variance between the CAD drawing and the optical measurement of the punch after the deep drawing tests

As mentioned in chapter 3, the climate chamber was not available for the curing of the punch, so the punch was put into a bag filled with water, to simulate necessary humidity level of 90%, and then laid in a heating chamber. As a result of this improvisation, the left part of the punch, marked red in Figure 4.4, was not submerged during the curing process. This proves the huge influence of the concrete's curing process on its wear resistance.

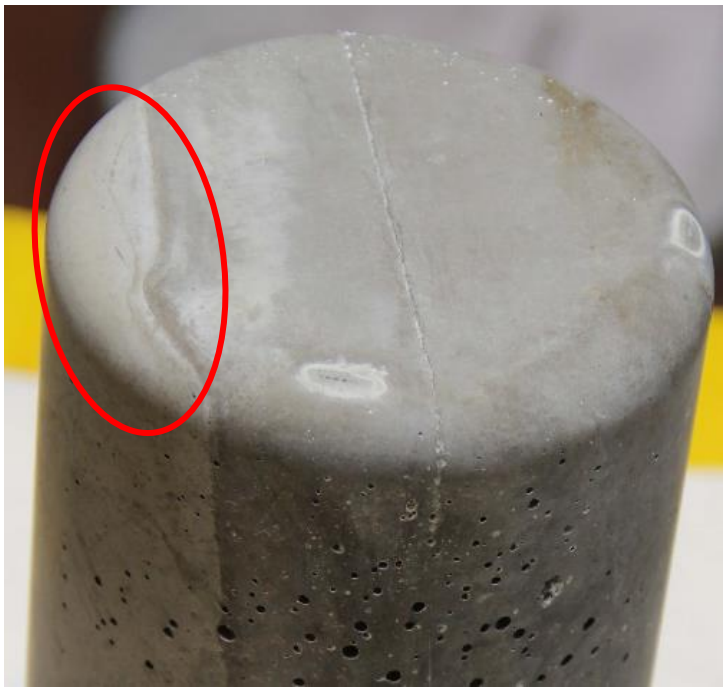

Figure 4.4: Punch 2 before the deep drawing tests

Figure 4.5: Punch 2 after the deep drawing tests

Furthermore, it is important to mention, that in comparison to the punch used in the preliminary tests the one used in primary tests did not show any visible abrasion during the tests (Figure 4.6). At the beginning of the preliminary tests the first punch already had steel fibers showing out of its cavities, which got hooked into the blank during the forming process causing the concrete crumble and fall off. The primary punch did not have these problems. Although there were abrasions on the radius area, even with some small cavities on this surface the concrete did not fall off in visible pieces during the deep drawing tests.

Figure 4.6: Punch 1 after the preliminary tests

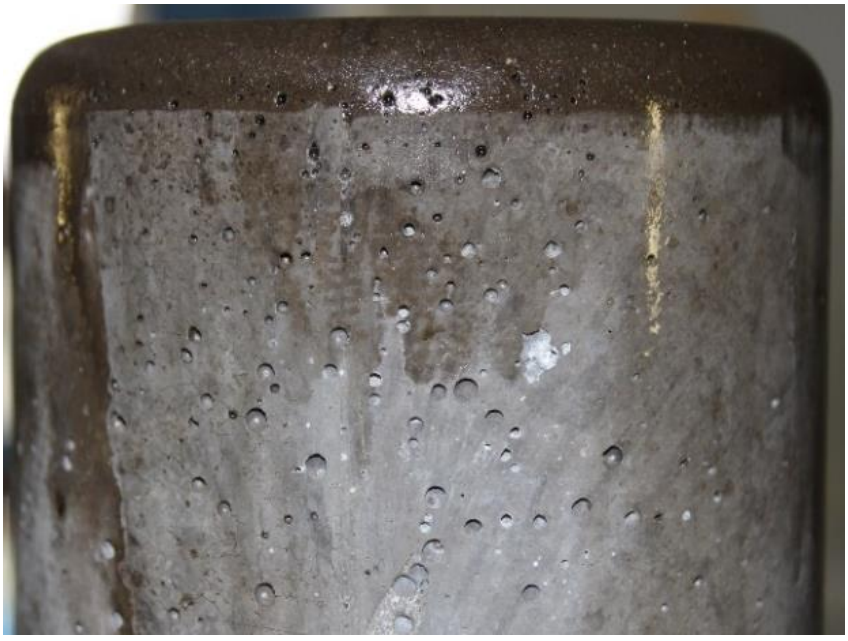

Figure 4.7: Punch 2 after the main tests

Additionally, as listed in Table 3.2, the concrete of the second punch has half the amount of steel fibers and a higher w/c value, but nearly the same Young's Modulus. Therefore, it is safe to say that, the main reason for the different behavior of the two

punches is the fibers pulling the concrete out of the punch during the deep drawing process.

4.1.1 Cost comparison

After the confirmation that UHPC can be used as a tool material it is necessary to look into the financial aspect of the punch's production. As mentioned in chapter 2, the production steps of a steel punch are, milling the wanted geometry out of a steel block, then hardening the material and performing the post processing operations. Because the investigated cup geometry can be produced very rapidly, the production costs of the steel and the concrete punch are nearly equal (cf. Table 4.2 and Table 4.3). Therefore, a comparison of the manufacturing costs of a more complex punch geometry (geometry shown in Figure 4.8) was conducted.

This punch was produced out of steel at the research group Tools and Forming for a different project. The punch had been produced in two parts, due to the demands of the former project. The concrete version of the punch was not produced. The calculation was done based on the values and experiences obtained during this thesis.

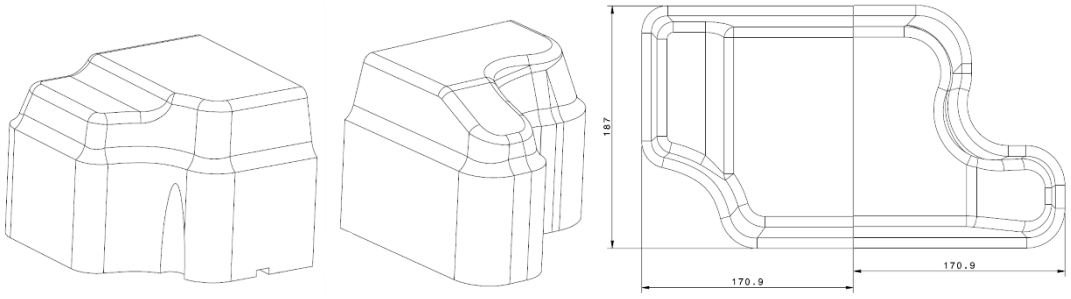

Figure 4.8: Drawing of the complex geometry

The concrete punch of the complex geometry is cast in the two parts as well, because otherwise the evenness of the flange cannot be guaranteed. The production of the mold is the most expensive step of the concrete punch production (Table 4.3), therefore the correct design of the mold is very important.

Table 4.2: Production costs of steel punches

Steel punch	Cup geometry	Complex geometry
Dimensions of the steel block and type of steel [mm]	150x150x500 mm (1.2379)	175x190x140 mm (1.2343, two times)
Material [€]	400	515
Pre-milling [€]	200	4,000
Hardening [€]	166	1,045
Post-processing [€]	234	4,875
Sum [€]	**1,000**	**10,435**
Break-even point [#]	100	348

Table 4.3: Production costs of UHPC punches

UHPC punch	Cup geometry	Complex geometry
Dimensions of concrete	Ø100x200 mm	341x187x132 mm (Figure 4.8)
Form (material + manufacturing) [€]	718	3,900
Flange (material + manufacturing) [€]	90	140
Concrete [€]	100	120
Curing [€]	150	200
Sum [€]	**1,058**	**4,360**
Break-even point [#]	106	146

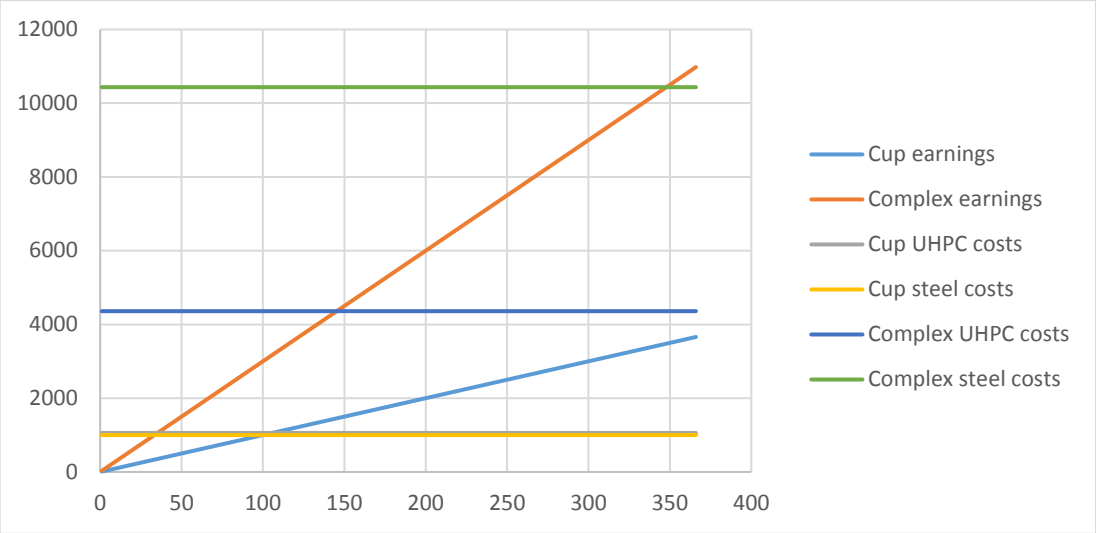

Figure 4.9: Break-even analysis of the different punches

A break-even analysis was done to show the effect on the costs when changing the geometry. Figure 4.9 depicts the results of the break-even analysis. The break-even point of the cup geometry is nearly the same for both production types (cf. Table 4.2 and
Table 4.3), but with a more complex geometry the break-even points are vastly different.

4.2 Evaluation of the blanks

For this project, it was necessary as well to compare the inner surface of the formed cups with those formed by a commonly used steel punch. Therefore, as mentioned in chapter 3, some tests were done with the available steel punch at the research group Tools and Forming. In Figure 4.10 the comparative steel sample is depicted, which was formed with the same process parameters as samples 16.1 – 20.10 (listed in Table 3.4).

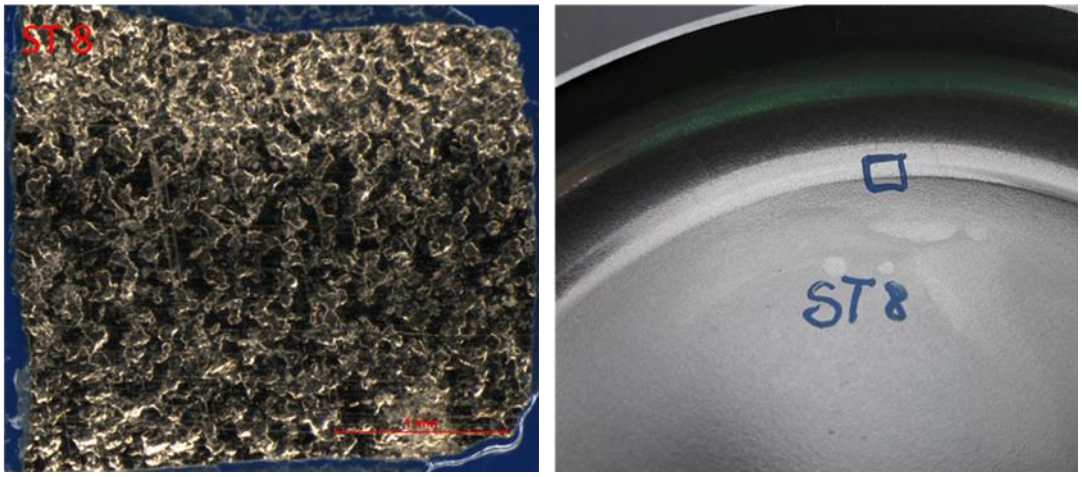

a) b)

Figure 4.10: Marked area of the blank, formed with the steel punch: a) under the microscope and b) on the blank

By virtue of the rotationally symmetricity of the cup's geometry only one sample area of the steel punch was necessary, which was different with the blanks formed by the concrete punch. In the second case, the separation joined made a mark on the blanks and the difference in the abrasion of the radius surface made additional investigation areas necessary. Figure 4.11 shows the chosen areas on the investigated specimens. As representatives of each group of the 6 parameter changes decided on in the DoE (listed in Table 3.4), the 10th (0.10), the 60th (5.10), the 110th (10.10), the 160th (15.10), the 210th (20.10) and the 260th (25.10) blanks were chosen.

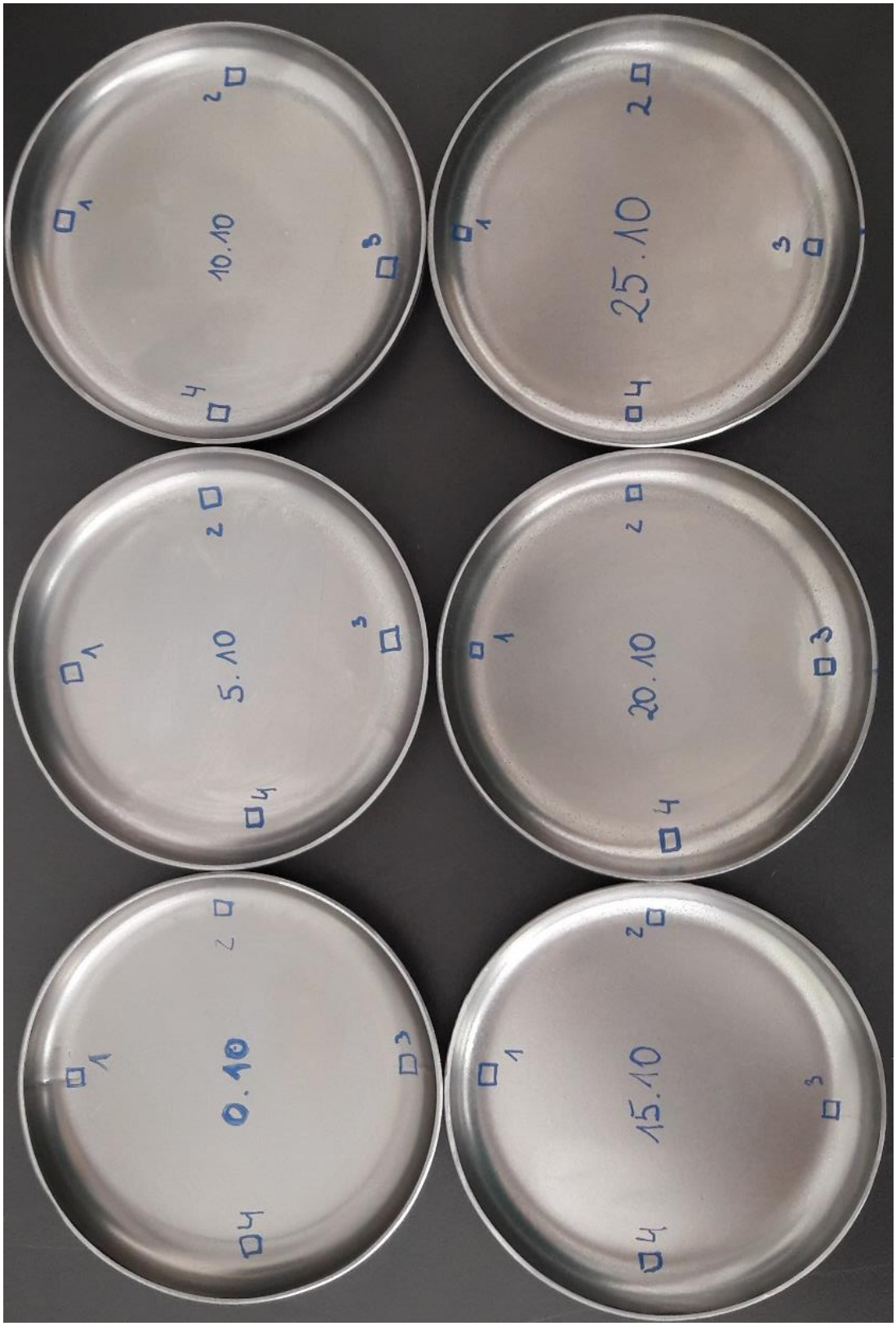

Figure 4.11: Investigated blanks with the chosen areas

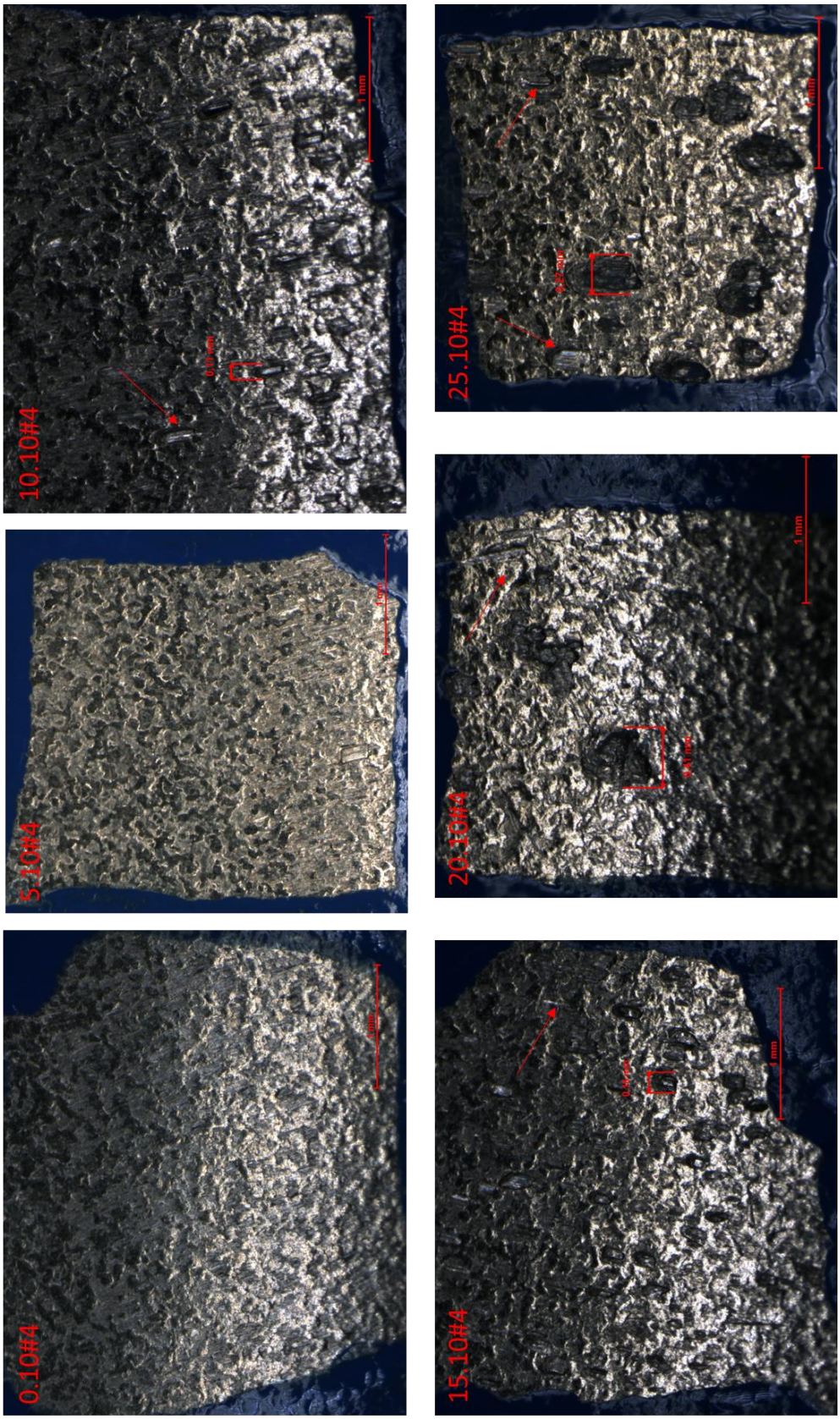

Figure 4.12: Area #4 under the microscope of the investigated blanks

The first visual inspection resulted in the discovery that the mark, made by the division joint (visible in Figure 4.11 blank 0.10 area 1), becomes less deep with further strokes and is nearly invisible after the 200th stroke. A further discovery was, that the holes made by the steel fibers of the punch were becoming more and more visible, starting from the 160th stroke, which is illustrated in Figure 4.11. The last effect, which is visible with bare eyes, is that the radius surface of the concrete punch produces a less smooth surface on the blank than the steel punch.

To investigate the effects of continuous wear of the concrete punch, area 4 of each specimen was chosen for comparison. Figure 4.12 shows those areas enlarged under the microscope. In contrast to the first (visual) investigation of the blanks, the microscope reveals that the wear of the concrete has started 50 strokes before the previous assumption. The first notches created by the steel fibers are present in the picture of the 110th stroke in Figure 4.12.

Another indicator of the increased abrasion of the concrete punch is the appearance of grooves, which are marked with red arrows in the pictures of Figure 4.12. These grooves are created by the fibers and they are oriented in the direction of the forming process.

5 Summary and outlook

5.1 Summary

Water, cement, silica fume, flow agent and quartz flour are the basic components of ultra-high-performance concrete. This concrete has a much denser microstructure as normal concrete and therefore it is much more resistant against high compressive strengths. When adding fine steel fibers of approximately 0.2 mm in diameter and 9 to 17 mm in length, even some small tensile strengths can be endured.

The small particle sizes make it possible for the concrete to replicate the finest structures of the mold surface. All these advantages make the material suitable for a sheet metal forming process, which was tested in this thesis.

The deep drawing process was chosen as a representative of the forming processes, to tryout the UHPC. The experiment was done with blanks made of a high strength steel, DC04, which is commonly used in the automotive industry. Therefore, the properties of this steel are well known and the focus of the investigation lay on the performance of the concrete.

Especially for the mechanical engineer the concrete's behavior was an unknown topic, with literature about this material also not providing many answers. Therefore, preliminary tests were necessary to find the right design of experiment. Furthermore a suitable method of investigating the surface of the punch without destroying it had to be found.

A structure analysis was performed to investigate the wear of the material. In the course of this investigation the concrete punch was 3D measured with the ATOS III system by the GOM GmbH before and after the tests to obtain the wear of the surface. In addition, the formed blanks were investigated under a light microscope made by Nikon to see the effects of the changing concrete surface on the inner surface of the formed steel blanks.

The final investigation of the punch was a break-even analysis of two different punch geometries. The objective of this examination was to find out if the concrete punch is more or less expensive in comparison to the same punch manufactured of steel, when making the punch's geometry more complex. The result of this analysis was, that the concrete itself does not influence the cost as much as the mold production.

Consequently, the concrete punch is comparatively less expensive the more complex the geometry is.

The objective of this thesis was to show if the brittle but strong material was suitable for prototyping of deep drawing parts in the automotive industry. Hence, after 260 trials with different deep drawing speeds the investigated punch shows no significant signs of wear and the quality of the formed blanks is also within the necessary tolerances. Thus, it can be said that the goal of this thesis was reached and UHPC has proven its potential.

5.2 Outlook

The next step is going to be the study of the results of the on-site test at the MAGNA Cosma Engineering Europe GmbH.

The chosen geometry was a simple one where none to small tensile strengths were transferred into the investigated concrete part. Thus, by virtue of the good performance of ultra-high-performance concrete, the next step for further investigate the concrete as a mechanical engineering material is to make the geometry of the test piece more complex.

The complex geometry investigation opens up the question about the financial advantages of the change in material. During the production of the simple geometry investigated in this thesis the in literature mentioned cost benefit of concrete compared to steel did not appear. The production costs for both versions of the punch were nearly the same, but the tendency of a cost reduction when using a more complex and bigger design did emerge during the experiment.

Not only the geometry of the concrete part has potential of improvement, the flange design is still very robust. The concrete has a nearly 70% lower density than steel, therefore the flange does not need to carry a lot of weight and can be made as light as possible, which also has a positive financial impact.

Another possible aspect that should be looked further into is the possibility of warm or even hot forming. During the literature research, it was mentioned that UHPC is very vulnerable to spalling because of high temperatures, but a possible cure for this problem was also found, polypropylene fibers. Even though those fibers can aide with spalling, they are reducing the compressive strength of the concrete. Therefore, the

recipe for the concrete mixture must be systematically changed to achieve the best suitable solution.

In addition to the changes in the concrete mix the curing process is also a process which can be reinvestigated. Because of the different results of abrasion on the radius surface of the punch, it is proven that curing has a big influence on the dimensional stability of the concrete.

In case of not only using the concrete for a prototype production but also for smaller series production, the possibility of a protective coating for the concrete surface is an additional subject that can be considered. As mentioned in the patent from the Spanish company, concrete can be cold or warm sprayed to apply a protective coating.

During this thesis only the deep drawing velocity and the drawing depth was altered, thus, this process also shows potential improvement. The small amount of abrasion indicates, that the blank material can be changed to a much harder one to find the maximum endurance of the concrete.

List of References

Bamonte, P. and Gambarova, P.: Properties of Concrete Subjected to Extreme Thermal Conditions
In: Journal of Structural Fire Engineering, Vol. 5 Iss 1 pp.47-62, Emerald Insight 2014

Bischoff, R.: Anlaufmanagement - Schnittstelle zwischen Projekt und Serie.
In: Götte, S. (editor.), Konstanzer Managementschriften: Band 2, 1.Auflage, Konstanz 2007

Dillinger, J. et al.: Fachkunde Metall, Europa-Lehrmittel 2007

Doege, E. and Behrens, B.-A.: Handbuch der Umformtechnik – Grundlagen, Technologien, Maschinen, Springer 2010

Fehling, E., et al.: Ultrahochfester Beton UHPC
In: Bergmeister, K., Fingerlos, F. and Wörner, J.-D. (editors), Beton-Kalender 2013: Lebensdauer und Instandsetzung-Brandschutz, Ernst & Sohn GmbH & Co. KG 2013

Fehling, E., et al.: Ultra-High Performance Concrete UHPC – Fundamentals, Design, Examples, Wilhelm Ernst & Sohn Verlag 2014

Fritz, A. H.: Umformen
In: Fritz, A. H., Schulze, G. (editors), Fertigungstechnik, Springer Vieweg 2015

Habig, K.-H. and Woydt, M.: Tribologie
In: Grote, K.-H. and Feldhusen, J. (editors), Dubbel - 24. Auflage, Springer 2014

Hoffmann, H. et al.: A new approach to determine the wear coefficient for wear prediction of sheet metal forming tools
In: Production Engineering, Volume 1, Issue 4, pp. 357-363, Springer 2007

Holmberg, K. and Matthews, A.: Tribology of Engineered Surfaces
In: Stachowiak, G.W. (editor), Wear – Materials, mechanisms and practice, John Wiley & Sons 2005

Hutchings, I.M.: The challenge of wear
In: Stachowiak, G.W. (editor), Wear – Materials, mechanisms and practice, John Wiley & Sons 2005

Kato, K.: Classification od Wear – Mechanisms/Models
In: Stachowiak, G.W. (editor), Wear – Materials, mechanisms and practice, John Wiley & Sons 2005

Kleiner, M., et al.: Development of ultra high performance concrete dies for sheet metal hydroforming
In: Production Engineering, Volume 2, Issue 2, Springer 2008

Klocke, F. and König, W.: Fertigungsverfahren 4 – Umformtechnik, Springer 2006

Li, W., et al.: Early-age shrinkage development of ultra-high-performance concrete under heat curing treatment
In: Construction and Building Materials 131 (2017) p. 767-774, Elsevier 2016

Lyons, A.: Materials for Architects and Builders (Third edition), Elsevier 2006

Moro, J. L., et al.: Baukonstruktion Grundlagen, Springer 2009

Sagmeister, B.: Maschinenteile aus zementgebundenem Beton, Beuth 2017

Schmidt, M.: Ultra-Hochleistungsbeton-Ausgangsstoffe, Eigenschaften und Leistungsfähigkeit
In: Schmidt, M., Fehling, E. (editors), Ultra-Hochfester Beton, Planung und Bau der ersten Brücke mit UHPC in Europa, Schriftenreihe Baustoffe und Massivbau, Heft 2, Kassel 2003

Schmidt, M., et al.: Sachstandsbericht: Ultrahochfester Beton, Deutscher Ausschuss für Stahlbeton, Heft 561, Beuth 2007

Schuler: Metal forming handbook, Springer 1998

Schwartzentruber, A., et al.: Hydraulic concrete as a deep-drawing tool of sheet steel
In: Cement and Concrete Research, Volume 29, Issue 2, Elsevier 1999

Siegert, K.: Kapitel 4, Tiefziehen
In: Siegert, K. (editor), Blechumformung - Verfahren, Werkzeuge und Maschinen, Springer 2015

Sommer, K. et al.: Verschleiß metallischer Werkstoffe – Erscheinungsformen sicher beurteilen, Springer 2014

Wang, R., et al.: Influence of the rheological properties of cement mortar on steel fiber distribution in UHPC
In: Construction and Building Materials 144 (2017) p. 65-73, Elsevier 2017

Westkämper, E. and Warnecke, H.-J.: Einführung in die Fertigungstechnik, Vieweg+ Teubner Verlag 2010

Zhao, S., et al.: Abrasion Resistance and Nanoscratch Behavior of an Ultra-High Performance Concrete
In: Journal of Materials in Civil Engineering 2017 29(2), American Society of Civil Engineers 2016

Weblinks

budestag.de: https://www.bundestag.de/blob/438002/42b9bf2ae2369fd4b8dd119d968a1380/wd-5-053-16-pdf-data.pdf (14.08.2017)

ductal.com: http://www.ductal.com/en/architecture/discover-ductal (14.03.2017)

feintool.com: https://www.feintool.com/fileadmin/user_upload/Produkte_Services/Pressen_Komplettsysteme/Services/Schmierstoffe_Broschuere_DE.pdf (18.08.2017)

history.tugraz.at: http://history.tugraz.at/main.php (14.08.2017)

meusburger.com: http://www.meusburger.com/en/standard-parts/material-grades/12343-12343-esr-hot-work-steel.html (24.03.2017)

oxforddictionaries.com: https://en.oxforddictionaries.com/definition/wear (19.08.2017)

rampf-gruppe.de: http://www.rampf-gruppe.de/uploads/media/WB-1404_TDS_DE.pdf (22.04.2017)

thyssenkrupp.at: http://www.thyssenkrupp.at/files/qs/TechnischeInfo/Feinblech%20und%20oberflaechenveredeltes%20Material/produktinformation_tiefziehstaehle_dd_dx_und_dc_de.pdf (22.04.2017)

tugraz.at: https://www.tugraz.at/arbeitsgruppen/tf/arbeitsgruppe-tf/ausstattung/ (22.04.2017)

US patent office: http://pdfaiw.uspto.gov/.aiw?PageNum=0&docid=20130183463&IDKey=C55AE37C760C&HomeUrl=http%3A%2F%2Fappft.uspto.gov%2Fnetacgi%2Fnph-Parser%3FSect1%3DPTO1%2526Sect2%3DHITOFF%2526d%3DPG01%2526p%3D1%2526u%3D%2Fnetahtml%2FPTO%2Fsrchnum.html%2526r%3D1%2526f%3DG%2526l%3D50%2526s1%3D20130183463.PGNR.%2526OS%3D%2526RS%3D (22.04.2017)

List of Figures

List of Tables